EXPERIMENTAL DETERMINATION OF AERODYNAMIC CHARACTERISTICS OF CYLINDRICAL AND SPHEROIDAL BODIES OF REVOLUTION

,2/1

A THESIS

Presented to

the Faculty of the Division of Graduate Studies

Georgia School of Technology

In Partial Fulfillment

of the Requirements for the Degree

Master of Science in Aeronautical Engineering

by

Robert Weaver Rainey

March 1948

EXPERIMENTAL DETERMINATION OF AERODYNAMIC CHARACTERISTICS OF CYLINDRICAL AND SPHEROIDAL BODIES OF REVOLUTION

Approved:

Date Approved by Chairman February 6, 1948

ACKNOWLEDGMENTS

The author wishes to express his sincerest thanks to Professor Hurlbut W. S. La Vier who suggested this thesis topic and for his valuable aid and guidance throughout its prosecution. The author also wishes to thank Professor G. K. Williams for his supervision and aid in operating and maintaining the equipment used and Mr. Olin Rogers for the excellent construction of the models tested.

The appreciation of the author is also extended to the Faculty of the Daniel Guggenheim School of Aeronautics, Georgia School of Technology, for their timely suggestions.

TABLE OF CONTENTS

PREFACE

MEANING OF SYMBOLS USED

A Maximum cross-sectional area of model, square feet

A_T Cross-sectional area of wind tunnel test-section, square feet

d Maximum diameter of model in inches

C_D Coefficient of drag = $\frac{D}{q\ A}$

C_L Coefficient of Lift = $\frac{L}{q\ A}$

C_M Coefficient of Moment about the center of gravity of the model = $\frac{M}{q\ A\ l}$

D'_o Initial drag setting on control-box vernier ($V = 0$)

D'_M Control-box vernier reading of drag during model runs

D'_T Control-box vernier reading of drag during tare runs

ΔD_M Increment of drag readings for models

ΔD_T Increment of drag readings for tare

D Drag of model (pounds) = $0.432\ (\Delta D_M - \Delta D_T)$

h_s Static pressure in test-section, millimeters of alcohol (sp. gr. = 0.816)

h'_s Static pressure in large section of wind tunnel up-

stream of test-section, millimeters of alcohol (sp. gr. = 0.816)

l Length of models, inches

L'_o Initial lift setting on control-box vernier (V = 0)

L'_M Control-box vernier reading of lift during model runs

L'_T Control-box vernier reading of lift during tare runs

ΔL_M Increment of lift readings for models

ΔL_T Increment of lift readings for tare

L Lift of models (pounds) = $1.05\ (\Delta L_M - \Delta L_T)$

M'_o Initial moment setting on control-box vernier (V = 0)

M'_M Control-box vernier readings of moment during model run

M'_T Control-box vernier readings of moment during tare run

ΔM_M Increment of moment readings for models $= (M'_M - M'_o)$

ΔM_T Increment of moment readings for tare $= (M'_T - M'_o)$

M Moment of model (foot-pounds) = $0.244 \times \frac{3}{12} \times (\Delta M_M - \Delta M_T)$

LIST OF TABLES

LIST OF FIGURES

FIGURE PAGE

FIGURE PAGE

EXPERIMENTAL DETERMINATION OF AERODYNAMIC CHARACTERISTICS OF CYLINDRICAL AND SPHEROIDAL BODIES OF REVOLUTION

I SUMMARY

A number of cylindrical bodies of revolution with bluff, conical, and hemispherical noses and spheroidal bodies of revolution were tested in the Thirty-Inch Wind Tunnel at The Daniel Guggenheim School of Aeronautics, Georgia School of Technology; all models tested were of the same maximum cross-sectional area; consequently, for a definite length/diameter ratio, every model had the same length and diameter.

The models were tested in an open-throat with a constant wind velocity of 97 feet per second, and the forces were measured by use of a strain gage balance system.

As a result of these tests it is possible to compare the relation of lift, drag, and moment of the various models in coefficient form.

II INTRODUCTION

A study of existing information on bodies of revolution indicated a general lack of experimental data on lift, drag, and moment with a variation of angle of attack and/or length/diameter ratio. The majority of the data available pretains primarily to the drag at zero angle of attack.

The study of pertinent data and literature revealed that the majority of basic bodies of revolution have unstable characteristics; however, the degree of their instability was not given. In addition, the problem of predicting analytically the forces and moment on a body of revolution has been limited not only by a lack of data that pertained to the different shapes under consideration but also by the lack of some practical analytical solution which could be applied to basic bodies of revolution and their related shapes.

The experimental comparison of lift, drag, and moment, therefore, has been undertaken and presented for the basic cylindrical and spheroidal bodies of revolution (see Figures 20-23). This data compares favorably with the limited data on hand at the present time and is presented as a means of comparing the aerodynamic characteristics. There is little doubt but that such information is important to the ballistician not only as a means of comparison but also as a basis for aiding in the prediction of the forces on bomb form

designs which might vary but slightly from the shapes of the models tested.

This information should be of interest to the aerodynamist and the aircraft designer because the fuselage, nacelles, and external gasoline tanks are similar to the models tested; and the effects of the fuselage on the performance of the complete airplane are becoming increasingly important.

III APPARATUS AND EQUIPMENT

In the initial investigation preceding this series of wind tunnel tests a consideration of the various types of wind tunnel test-sections was made with the purpose of selecting a test-section which would yield the desired results with a minimum of corrections. Whenever a wind tunnel is used to obtain the experimental aerodynamic characteristics of a model, several tares and corrections must be applied to the "raw" data to convert it to correct and usable data. Briefly, the corrections are:

1. To account for the non-uniformity of flow in the test-section
2. The effect of the support system on the model
3. The effect of the model on the support system
4. Tunnel wall or jet-boundry effects
5. Interference effects between model and support
6. Blocking effects
7. Effect of supports and balance system

An open-throat test-section was decided upon; for despite the divergence of flow in the test-section, the jet-boundry effects, longitudinal static-pressure gradient[1], and

---

[1]Herman Glauert, "The Effect of the Static Pressure Gradient on the Drag of a Body Tested In a Wind Tunnel," Technical Report of the Aeronautical Research Committee (British), Vol. I, Reports and Memoranda No. 1158, 1928-29, pp. 91-92.

blocking effects are negligible because of the lack of test-section walls. Therefore, the Thirty-Inch Wind Tunnel was used with an open-throat test-section.

The models were constructed of redwood with a $1\frac{1}{2}$-inch diameter so that with a large length/diameter ratio the model would not extend beyond the test-section. The models were first slotted at the centerline in the vertical plane at the center of gravity and three inches behind the center of gravity so that a conventional type of mounting could be used (see Figure 2). This method of mounting proved unsatisfactory, and the models were modified so that they could be offset from the balance system supports (see Figures 2 and 17). Thus, the models were mounted beyond the flow that was disturbed by the supports, fairing, and mounts of the balance system. Since every model was mounted with the front support at the center of gravity, the moment about the center of gravity was measured directly (see Figure 1). By use of this type of mount it was possible to measure tares without the use of dummy system.[2]

The forces were measured by use of a strain gage balance system controlled by a Baldwin-Southwart SR-4

---

[2]R. S. Swanson, and C. L. Gillis, Wind-tunnel Calibration and Correction Procedures for Three-dimensional Models, U. S. National Advisory Committee for Aeronautics, Wartime Report L-1, October, 1944, p. 11.

Control Box and a twenty-pole selector box.[3] The power was furnished by a six-volt automobile storage battery and kept in a charged condition by use of a rectifier. By using the selector box it was possible to read the lift, drag, or moment forces without changing any connections. It was found that after becoming familiar with the testing procedure, a complete series of test-runs on one model could be accomplished in one and one-half hours.

The wind tunnel was controlled with a radial type variable resistor and a sliding type variable resistor in series to accomplish more minute adjustments in wind velocity.

It was found that when the wind velocity exceeded 97 feet per second, the vibration of the tunnel and adjoining control-box was excessive and that it was impossible to take accurate readings. Despite the fact that efforts were made to eliminate the detrimental effects of vibration by mounting the control-box on rubber vibration absorbers, all efforts proved unsatisfactory; and the wind velocity was limited to 97 feet per second.

All of the models were tested with a variation of

---

[3]Leslie R. Merritt, The Development of a Strain Gage Balance System for the Thirty Inch Wind Tunnel at the Georgia School of Technology, unpublished thesis in partial fulfillment of the requirements for the degree Master of Science in Aeronautical Engineering, Daniel Guggenheim School of Aeronautics, George School of Technology, June, 1947.

angle of attack of from -9 degrees to +9 degrees. The angles were set to an accuracy of 1/20 of one degree by use of bubble inclinometer.

IV PROCEDURE

Before any preliminary test runs were made with models mounted on the balance system, a velocity and inclination survey was made of the empty open-throat test-section in the vicinity of where the model would be mounted. This survey was accomplished by use of a calibrated directional pitot tube (yawhead) which was mounted in the test-section by use of an overhead rail system[4]. Upon maintaining a velocity of 97 feet per second at the longitudinal centerline of the test section, the average longitudinal velocity gradient was found to be so small that the change in velocity in the vicinity of where the model was mounted was approximately one foot per second or approximately a one percent change. The lateral change in velocity was found to be negligible due to the small diameter of the model.

The inclination of the air stream was determined and found to be 0.25 degrees upflow at the center of the test-section. The change of upflow along the longitudinal axis was found to be negligible due not only to the lack of change in direction of the air stream but also to the

---

[4]R. W. Rainey, The Design of a Directional Pitot Tube Attachment for Open Throat Wind Tunnels, August 1947, unpublished student technical report deposited in the Library of the Daniel Guggenheim School of Aeronautics, Georgia School of Technology.

inability of the directional pitot tube to indicate the flow inclination more accurately than to the nearest 0.25 degrees.[5]

The turbulence factor was determined by use of a $4\frac{1}{2}$-inch sphere and was estimated by extrapolation to be 1.30 with three screens installed in the large section of the tunnel upstream of the converging section. Comparison with other experimental data indicates the possibility of an even lower turbulence factor -- in the range of 1.10 - 1.15 -- however, 1.30 was chosen as a conservative approximation and will make no difference in the final results. This is relatively a low turbulence factor and is substantiated by the uniformity of velocity along the longitudinal centerline of the test-section.[6]

The directional pitot tube was used to determine the static pressure gradient along the tunnel centerline in the vicinity of the model mounts. As could be expected for an open-throat wind tunnel, the static pressure was constant and equal to the atmospheric pressure throughout the section investigated.

Despite the fact that there is a small longitudinal dynamic pressure gradient caused by models that are not

---

[5]Swanson and Gillis, op. cit., p. 14.

[6]Swanson and Gillis, ibid., p. 10.

aerodynamically clean[7], calculations indicate that the gradient is exceptionally small in an open-throat test-section as compared to the gradient in a closed jet[8]. This smallness is accentuated by the fact that the maximum cross-sectional area of the models, A, were 0.01226 square feet as compared to a jet cross-sectional area, A_T, of 6.25 square feet resulting in an exceedingly small ratio of $A/A_T = 0.00195$. It was therefore possible to neglect the longitudinal dynamic pressure gradient in all calculations of the forces on the model.

In the preliminary test runs the models were mounted in a conventional manner with the two supports of the balance system extending through the lower portion of the models, and the model was attached to the ball-bearings in the end of the supports by 1/8-inch diameter pins (see Figure 2). This method of mounting proved unsuccessful because the supports induced interference along the lower surface of the model downstream of the supports. The interference in turn spoiled the pressure distribution of the lower portion of the model resulting in the lift not being zero at zero angle of attack, and at plus and minus angles of attack the lift curves were not symmetrical.

---

[7] Loc. cit.

[8] Herman Glauert, "Wind Tunnel Interference on Wings, Bodies, and Airscrews," Technical Report of the Aeronautical Research Committee (British), Reports and Memoranda No. 1566, 1933.

Even though a dummy system was used to determine tares, it proved unsatisfactory. That configuration induced inherent difficulties of proper alignments and clearances between the dummy support and the model. Other difficulties in obtaining the tares were that the drag tares were of the same magnitude as the total drag of the model itself (which would result in a large percentage of error in the drag of the model), a large number of test runs would have had to been made thereby adding to the possibilities of human and operational errors, and the tares for lift and moment would not correct the data of the model test runs due to the large change in pressure distribution over the surfaces of the model.

After a substantial number of preliminary test runs were made with the conventional mount, that type of mount was abandoned; and other types of mounts were considered. Because the models were to be tested at different angles of attack, it was necessary to attach the model so that a plane passed through the model supports would be perpendicular to its plane of rotation. To pitch the model in a vertical plane, the mounts had to enter the model from the side in a horizonal plane thereby reducing the effects of interference on the model. This was accomplished by use of rods which permitted the model to be offset from the original mounting supports of the balance system. Drill

rod of 1/8-inch diameter was chosen to offset the models, and the models were drilled at the center of gravity and three inches behind the center of gravity to receive the drill rods.

Two ball bearings were later placed in the models at the center of gravity to reduce the moments set up by friction as well as to align the model properly while on the mount. In the case of the models with $l/d = 2$, an extension had to be attached to the rear of the models so that a distance of three inches could be maintained between front and rear supports, thereby clearing the rear support of the balance system fairing (see Figure 17).

The position of the balance system was arranged so that the centerline of the model at zero angle of attack would coincide with the longitudinal centerline of the test-section (see Figure 18), and the models would be mounted within the surveyed section of the jet.

In the test runs the models were first placed at zero relative angle of attack by mounting the models onto the drill rods and adjusting the length of the rear support until the actual angle of the model was at -0.25 degrees[9] (see Figures 1 and 17). The control-box vernier readings for lift (L'_o), drag (D'_o), and moment (M'_o) were taken. The

---

[9] Cf. ante., p. 8.

tunnel was then started, and the velocity in the test-section held at a constant 97 feet per second by use of a bottle manometer reading the static pressure (h'_s) in the large section of the tunnel upstream of the converging nozzle (see Figures 18 and 19). Calibration of the velocity in the test-section, V, versus h'_s indicated that for V = 97 feet per second, h'_s = 71.6 millimeters of alcohol.

While maintaining a constant velocity the vernier readings of the forces on the models were taken, i.e., L'_M, D'_M, and M'_M. After repeat vernier readings were taken with the tunnel in operation, the tunnel was then shut down; and repeat readings of L'_o, D'_o, and M'_o coincided within experimental accuracy with the initial vernier readings.

Similar runs were then made from -9 degrees to +9 degrees in increments of 3 degrees. During all runs the velocity was maintained constant at 97 feet per second, and repeat runs at zero relative angle of attack and at one other angle of attack were made to substantiate the validity of the tests.

Tare runs were made in a similar manner with only the balance system and supports mounted in the test-section. This configuration was similar to that with which the model runs were made except that the model was removed. The initial readings for tare runs were taken as before with V = 0 and recorded as L'_o, D'_o, and M'_o; with V = 97 feet per

second, lift, drag, and moment readings were recorded as L'_T, D'_T, and M'_T. The rear vertical support was varied in length to coincide with a variation of relative angle of attack, the same as though a model was mounted in place.

The analysis of tare data[10] showed a variation of tare for drag due to the variation in length of the rear support but a constant tare equal to zero for the lift readings. The moment tare indicated a negative initial tare for $\alpha = 0$ and very little variation of tare for a variation in α.

Because the model was directly supported by 1/8-inch diameter drill rods, the effects on tare by interference due to the intersection of support rods and model could be neglected. This would not be true in the case of a model with large support members; however, the support rods were small and of a circular cross-section. The complexities of determining these interference effects on the model would have more than offset the very small error involved in neglecting them entirely.

For the reduction of the control-box vernier readings into lift, drag, and moment, the balance system was calibrated;[11] and a plot of vernier reading versus applied load

---

[10] Alan Pope, Wind-Tunnel Testing, (New York: John Wiley and Sons, Inc., London: Chapman and Hall, Ltd., 1947), p. 124.

[11] Ibid., p. 119.

in pounds was plotted. The slope of each curve was found to be constant throughout the calibration range, and they were found to be:

Lift strain gage = 1.05 pounds/unit vernier reading

Drag strain gage = 0.432 pounds/unit vernier reading

Moment strain gage = 0.244 pounds/unit vernier reading

It is to be noted that the strain gage attached to the rear support measured the force caused by the moment about the center of gravity of the model, and the moment about the center of gravity is the product of that force and the lever arm through which the force was acting. In these model tests the lever arm is always the distance between the two supports (three inches).

Therefore, to convert the raw data into the forces on the model, the tare was subtracted from the vernier reading and the remainder multiplied by the slope of the respective strain gage calibration curve. For the moment calculations the force on the rear support was multiplied by the lever arm of three inches. To further convert the data into coefficient form the lift and drag were divided by the product of the cross-sectional area and dynamic pressure and the moment divided by the product of the dynamic pressure, cross-sectional area, and the length of the model. The coefficients were then plotted versus angle of attack for each model and are presented in the appendix of this thesis.

V RESULTS AND ANALYSIS

Due to the lack of experimental data on the aerodynamic characteristics of shapes of revolution, it was difficult to compare the present data with that of previous wind tunnel tests on such shapes. However, there is a limited amount of data on the drag of flat plates, spheres, and cylinders with bluff noses at zero angle of attack.[12]

It is difficult to determine the actual Reynolds numbers of the models tested because in disc and sphere tests, the diameters are used as the linear dimension, and in airfoil studies the chord is used as the linear dimension. Therefore, it would be hard to correlate the Reynolds numbers of a series of bodies of revolution whose diameters remain constant and lengths vary to those of two-dimensional or three-dimensional tests. The range of Reynolds numbers in these tests -- dependent upon the length of the models -- varied from 201,000 to 1,004,000.

The small effect of Reynolds number upon the total drag of a shape of revolution can be illustrated. The total drag is approximately equal to the sum of the pressure drag -- which is only slightly effected by a Reynolds number -- and the skin-frictional drag -- which

---

[12] G. Eiffel, The Resistance of the Air and Aviation, (London: Constable and Company, Ltd., Boston: Houghton Mifflin Company, 1913).

does vary with Reynolds number. A variation of Reynolds number will effect skin-frictional drag much more than it will the pressure drag, and it can be shown that the skin-frictional drag is only a small percentage of the total drag. Therefore, a change in skin-frictional drag by a variation of Reynolds number will cause only a very small change in the total drag.

For example, a bluff cylindrical body of revolution with $l/d = 2$ has a drag coefficient, C_D, equal to 0.82 at zero angle of attack (see Table I). The total drag of the model:

$$D = C_D qA$$
$$= 0.82 \times 10.70 \times 0.01226$$
$$= 0.1074 \text{ lbs.}$$

The relation of skin-frictional drag coefficient to Reynolds number is[13]:

$$C_F = \frac{0.455}{(\log_{10} R)^{2.58}}$$

---

[13] J. C. Hunsaker and B. G. Rightmire, Engineering Applications of Fluid Mechanics, (New York and London: McGraw-Hill Book Co., Inc., 1947), p. 193.

For a model with l/d = 2:

$$d = 1.5 \text{ inches}$$
$$l = 3.0 \text{ inches}$$
$$R = \frac{V\,l}{\nu} = \frac{97 \times 3/12}{0.000157} = 154{,}100$$
$$R_e = \text{T.F.} \times R = 1.3 \times 154{,}000 = 201{,}000$$

where ν = Kimematic viscosity
R = Measured Reynolds number
R_e = Effective Reynolds number
T.F. = Turbulence factor

$$C_F = \frac{0.455}{(\log_{10} 201{,}000)^{2.58}}$$
$$0.00614$$
$$D_F = C_F q A_W = 0.00614 \times 10.70 \left(\pi \times \frac{1.5 \times 3}{144}\right)$$
$$= 0.00643 \text{ lbs.}$$

where A_W = Wetted area of model parallel to wind

The relation of skin-frictional drag to total drag becomes $\frac{0.00643}{0.1074} = 0.0598$ or 5.98%. Therefore, a variation in Reynolds number -- or its method of computation -- would not effect the total drag appreciably since the skin-frictional drag is such a small percentage of total drag.

A comparison of the drag coefficients of cylinders with bluff noses at zero angle of attack obtained from these tests with those arrived at by G. Eiffel is presented in Figure 16, and the comparison indicates close agreement throughout the range of length/diameter ratios with the

exception of the flat plate ($l/d \cong 0$).

The comparative difference is due to the subject tests having been conducted in a wind tunnel with a higher Reynolds number, less turbulence, and a more accurate balance system. Had those factors been more nearly equal in the two tests, it is probable that there would have been closer agreement between the flat-plate drag coefficients. Present-day experiments[14] indicate flat-plate drag coefficients of about 1.25. Therefore, the drag coefficient for a flat plate in these tests is in the immediate range of present-day flat-plate drag coefficients.

Further analysis of Figure 16 reveals that the minimum drag of cylinders with bluff noses is evident with an $l/d = 2.3$ as compared with $l/d=2.5$ as arrived at by Eiffel. It may therefore be concluded that up to a length of 2.3 times the diameter, the body of revolution tends to straighten the flow in such a manner as to reduce the form drag more rapidly than the skin friction drag increases. As the l/d ratio increases beyond 2.3, the additional increase in length will increase the skin friction thereby increasing the total drag.[15]

---

[14] Alan Pope, "Letters to the Editor", Journal of the Aeronautical Sciences, Vol. 14, No. 11, November, 1947, p. 626.

[15] S. Goldstein, Modern Developments in Fluid Mechanics, (Oxford at the Clarendon Press, 1938) Vol. II, p. 507.

When the angle of attack of each model is varied the drag coefficient increases due to the increase in frontal area presented to the free stream, and the increase in turbulent flow past the body. For small angles of attack the pressure drag caused by the bluff nose remains fairly constant, but the form drag increases rapidly. Also evident from Figure 3 is the difference in the relative slopes of the drag curves, $\frac{dC_D}{d\alpha}$, for each model. Obviously, the longer models would have the higher values of $\frac{dC_D}{d\alpha}$ because of the greater frontal areas being presented to the free stream resulting in higher turbulence and form drag.

The lift coefficients of bluff cylinders are presented in Figure 4. Since the coefficients were based upon the maximum cross-sectional area of the model rather than the projected area as used in airfoil work, the lift coefficients increased with an increase in l/d at each angle of attack greater than zero. Apparently the maximum normal force was never reached since the slope of the lift curves are positive for all angles of attack.

In the determination of the moment coefficients it was anticipated that all bodies of revolution would be statically and dynamically unstable about their centers of gravity; however, the moment coefficients of bluff cylinders with l/d's of 2 and 4 indicate static stability within the

range of ± 10 and ± 4½ degrees angle of attack respectively (see Figure 5). This does not necessarily mean that a homogeneous body of revolution with a bluff nose and an $l/d < 4$ would fall through free space without tumbling. Instead it does indicate that at small angles of attack the "airprow region" and turbulence set up by the bluff nose causes the free stream to flow around the turbulent region and strike the model aft of the turbulent area presenting smooth flow over a portion of the after-body of the model. This in turn results in the center of pressure being aft of the center of gravity until $\alpha = 4\frac{1}{2}^{\circ}$ for $l/d = 4$ or $\alpha = 10^{\circ}$ for $l/d = 2$. With all models of $l/d > 4$ the center of pressure is forward of the center of gravity and moves further forward as α increases positively or negatively.

In the case of the cylindrical models with conical and hemispherical noses the drag coefficients are progressively smaller, not only because of the reduction of pressure drag at the nose but also because of the reduction of the turbulent flow past the model.[16] At zero angle of attack minimum drag coefficients are realized with models of $l/d = 3.6$ for conical noses and $l/d = 4.3$ for hemispherical noses, and the plot of drag coefficients versus l/d

---

[16] Ibid., Vol. II, p. 505

indicates a similarity between the two models with respect to their drag characteristics (see Figure 16). However, the models with the hemispherical noses have a drag of approximately one-half that of the models with conical noses probably due to a further reduction of turbulent flow within the boundry layer aft of the nose and reduction in form drag.

The lift curves for cylinders with conical noses (see Figure 7) indicate that the lift changes proportionally with angle of attack. This is not true for the shorter cylinders with hemispherical noses, but the slope of the longer two models is fairly constant (see Figure 10).

The analysis of the moment curves for cylinders with conical and hemispherical noses (see Figures 8 and 11) shows the effect of turbulence at the nose on the stability of a body of revolution. The cylinders with conical noses have higher drag coefficients and more turbulence near the nose caused by the abrupt change in shape at the junction of the conical and cylindrical portions of the model. Here again (as in the case of bluff cylinders) the test results of the shorter models indicate less unstable moments. The change from conical to hemispherical noses reduces turbulence near the nose -- thereby reducing the pressure drag -- resulting in a forward movement of the center of pressure and an increase in the positive slope of the moment curves

(see Figure 11). This decrease of turbulence in a compressible fluid flowing around the forward portion of a sphere (in this case a hemispherical nose) is substantiated by sphere tests in air.[17]

The plot of drag coefficients for the spheroids (see Figure 12) indicates a definite reduction in drag, this time the minimum drag coefficient being 0.098 at $l/d = 5.80$. Here again the slope of the drag curves becomes greater as the l/d ratio increases. The plot of drag coefficient versus l/d ratio -- Figure 15 -- shows the relationship of the drag coefficients for all models at zero angle of attack, that of the spheroids being the least. The characteristic shape of a spheroid is such that the pressure drag and turbulence are reduced by the lack of bluff ends on the model.

For spheroids with $l/d < 5.8$ the pressure drag increases faster than the skin friction is reduced resulting in an increase in total drag. Conversely, for spheroids with $l/d > 5.8$ the skin friction increases faster than the reduction of pressure drag, and again the total drag increases.

When the $l/d = 1$ the spheroid becomes a sphere;

---

[17] A. Wiley Sherwood, Aerodynamics, (New York: McGraw-Hill Book Company Inc., 1946), First Edition, pp. 98-102.

tests were not conducted on spheres in this series of runs, but it is interesting to note that the drag coefficient of a sphere -- which varies as the Reynolds number -- fairs in nicely with the drag curves of spheroids at zero angle of attack (see Figure 15).

The increase in pressure drag near the noses of the shorter models is not only indicated by the drag curves but is also upheld by the flattening of the moment curves as the l/d decreases -- especially in the case of Model I where l/d 2. It is believed that the reflex in the moment curve of Model I is exaggerated due to the difficulty in obtaining the moment tare of that model. However, regardless of this exaggeration, the relative shapes of the five moment curves uphold the indication of a rearward movement in the center of pressure by an increase in turbulence near the noses of the models as the l/d ratio decreases.

Test results show a reflex in the lift curves of spheroidal bodies of revolution that seems erroneous at first glance. It was found, however, that the lift curves of airship models with tapered tails tested in the open-throat tunnel at N.A.C.A., Langley Field, Virginia,[18] were

---

[18]Ira H. Abbott, Airship Model Tests in the Variable Density Wind Tunnel, U. S. National Advisory Committee for Aeronautics, Technical Report No. 394, 1931.

reflexed; and repeat runs of the spheroidal bodies of revolution were made that substantiated the results obtained in the first test runs.

VI CONCLUSIONS

1. The lower the drag coefficients of a family of bodies of revolution the higher the length/diameter ratio at which minimum drag occurs.

2. The amount of turbulent flow at or near the nose of a body of revolution has a decided effect upon the drag and moment of the body--greater turbulence caused by the nose increases the drag and decreases the unstable moment of the body.

3. A variation in the nose of a body of revolution has more effect on the drag and moment than on the lift. The degree of taper of a conical nose as well as the shape of the after-portion of the body varies the aerodynamic characteristics considerably.

4. In the design of a wind tunnel mount for bodies of revolution it is especially important to hold tares and interference to a minimum; otherwise, accurate and symmetrical results will not be obtained.

5. Within reasonable limits the surface roughness of all models tested should be the same, preferably a smooth, polished surface.

6. Further study of the effects of Reynolds number upon the aerodynamic characteristics of bodies of revolution would undoubtly prove valuable.

BIBLIOGRAPHY

Abbott, Ira H., Airship Model Tests in the Variable Density Wind Tunnel. U. S. National Advisory Committee for Aeronautics, Technical Report No. 394, 1931, 24 pp.

Eiffel, G., The Resistance of the Air and Aviation. London: Constable and Company, Ltd., Boston: Houghton Mifflin Company, 1913. 242 pp.

Glauert, Herman, "The Effect of the Static Pressure Gradient on the Drag of a Body Tested In a Wind Tunne." Technical Report of the Aeronautical Research Committee (British), Vol. I, Reports and Memoranda No. 1158, 1928-29. pp. 81-92.

_____, "Wind Tunnel Interference on Wings, Bodies, and Airscrews." Technical Report of the Aeronautical Research Committee (British), Reports and Memoranda No. 1566, 1933.

Golstein, S., Modern Developments in Fluid Mechanics. Oxford at the Clarendon Press, Vol. II, 1938. 702 pp.

Hunsaker, J. C., and B. G. Rightmire, Engineering Applicat- of Fluid Mechanics. New York and London: McGraw-Hill Book Company, Inc., First Edition, 1947. 494 pp.

Merritt, Leslie R., The Development of a Strain Gage Balance System for the Thirty Inch Wind Tunnel at the Georgia School of Technology. Unpublished thesis in partial fulfillment of the requirements for the degree Master of Science in Aeronautical Engineering, Daniel Guggenheim School of Aeronautics, George School of Technology, June, 1947. 40 pp.

Pope, Alan, "Letters to the Editor." Journal of the Aeronautical Sciences, Vol. 14, No. 11, November, 1947. pp. 626-627.

_____, Wind-Tunnel Testing. New York: John Wiley and Sons, Inc., London: Chapman and Hall, Ltd., 1947.

Rainey, R. W., The Design of a Directional Pitot Tube Attachment for Open Throat Wind Tunnels. Unpublished student technical report deposited in the Library of the Daniel Guggenheim School of Aeronautics, Georgia School of Technology, August 1947. 18 pp.

Sherwood, A. Wiley, Aerodynamics. New York: McGraw-Hill Book Company, Inc., First Edition, 1946. 220 pp.

Swanson, R. S., and C. L. Gillis, Wind-tunnel Calibration and Correction Procedures for Three-dimensional Models. U. S. National Advisory Committee for Aeronautics, War-time Report L-1, October, 1944. 45 pp.

APPENDIX I

SAMPLE CALCULATIONS

Using the cylindrical body of revolution with the bluff nose as an example[19]:

$\alpha = 9^{\circ}$ $\quad T = 75^{\circ}$

$V = 97$ feet per second $\quad P = 29.92$ inches Hg.

$A = 0.01226$ sq. ft.

$$\rho = \rho_{\circ} \times \frac{P}{P_o} \times \frac{T_o}{T} = 0.002378 \times \frac{29.32}{29.92} \times \frac{519}{534}$$

$= 0.00226$ slugs per cubic feet

$$q = \frac{\rho}{2} V^2 = \frac{0.00226}{2} (97)^2 = 10.70 \text{ lbs. per sq. ft.}$$

$L_o' = 7.050$

$L_M' = 7.082$

$\Delta L_M = L_M' - L_o' \quad 7.082 - 7.050 \quad 0.032$

$\Delta L_T = 0$ (From tare data)

$\Delta L_M - \Delta L_T = 0.032 - 0 = 0.032$

$L = 1.05 \times 0.032 = 0.0336$ lbs.

$$C_L = \frac{L}{q \times A} = \frac{0.0336}{10.70 \times 0.01226} = 0.253$$

---

[19] Cf. ante., pp. 14f.

$D'_o = 8.145$

$D'_M = 8.900$

$\Delta D_M = 8.900 - 8.145 = 0.755$

$\Delta D_T = 0.435$ (From tare runs)

$\Delta D_M - \Delta D_T = 0.320$

$D = 0.432 \times 0.320 = 0.138$ lbs.

$$C_D = \frac{D}{q \times A} = \frac{0.138}{10.70 \times 0.01226} = 1.06$$

$M'_o = 6.482$

$M'_M = 6.436$

$\Delta M_M = 6.436 - 6.482 = -0.046$

$\Delta M_T = -0.080$ (From tare runs)

$\Delta M_M - \Delta M_T = -0.046 - (-0.080) = 0.034$

$M = 0.244 \times 0.034 \times 3/12 = 0.0021$ ft. lbs.

$$C_M = \frac{M}{q \times A \times l} = \frac{0.0021}{10.70 \times 0.01226 \times \frac{6}{12}} = 0.0308$$

Similar calculations were carried out for all models at each angle of attack and recorded in the tables in Appendix II . Curves were then plotted and presented in Appendix III .

APPENDIX II

TABLES

TABLE I

AERODYNAMIC CHARACTERISTICS

CYLINDRICAL BODIES OF REVOLUTION

BLUFF NOSES

α	l/d = 2			l/d = 4			l/d = 6			l/d = 8			l/d = 10		
	C_L	C_D	C_M	C_L	C_D	C_M	C_L	C_D	C_M	C_L	C_D	C_M	C_L	C_D	C_M
0	0	.820	0	0	.878	0	0	.929	0	0	.966	0	0	.991	0
3	.095	.865	-.032	.103	.921	-.029	.125	.979	.0055	.143	1.020	.0062	.150	1.059	.0080
6	.180	.926	-.052	.192	.984	-.031	.240	1.045	.0161	.291	1.096	.0234	.315	1.137	.0303
9	.244	.995	-.066	.253	1.060	.031	.332	1.120	.0452	.446	1.178	.0523	.507	1.222	.0675
-3	.095	.865	-.032	.103	.921	-.029	.125	.979	.0055	.143	1.020	.0062	.150	1.059	.0080
-6	.180	.926	-.052	.192	.984	-.031	.240	1.045	.0161	.291	1.096	.0234	.315	1.137	.0303
-9	.244	.995	-.066	.253	1.060	.031	.332	1.120	.0452	.446	1.178	.0523	.507	1.222	.0675

TABLE II

AERODYNAMIC CHARACTERISTICS

CYLINDRICAL BODIES OF REVOLUTION

CONICAL NOSES

α	1/d 2			1/d 4			1/d 6			1/d 8			1/d 10		
	C_L	C_D	C_M	C_L	C_D	C_M	C_L	C_D	C_M	C_L	C_D	C_M	C_L	C_D	C_M
0	0	.484	0	0	.474	0	0	.494	0	0	.530	0	0	.572	0
3	.103	.517	.0018	.116	.501	.0037	.127	.550	.0111	.135	.595	.0171	.143	.658	.0185
6	.206	.559	.0037	.230	.589	.012	.262	.635	.034	.278	.687	.045	.286	.769	.050
9	.318	.605	.0083	.349	.687	.031	.381	.726	.062	.413	.782	.072	.437	.883	.0867
-3	.103	.517	.0018	.116	.501	.0037	.127	.550	.0111	.135	.595	.0171	.143	.658	.0185
-6	.206	.559	.0037	.230	.589	.012	.262	.635	.034	.278	.687	.045	.286	.769	.050
-9	.318	.605	.0083	.349	.687	.031	.381	.726	.062	.413	.782	.072	.437	.883	.0867

TABLE III

AERODYNAMIC CHARACTERISTICS

CYLINDRICAL BODIES OF REVOLUTION

HEMISPHERICAL NOSES

α	1/d 2			1/d 4			1/d 6			1/d 8			1/d 10		
	C_L	C_D	C_M	C_L	C_D	C_M	C_L	C_D	C_M	C_L	C_D	C_M	C_L	C_D	C_M
0	0	.229	0	0	.219	0	0	.226	0	0	.255	0	0	.311	0
3	.0556	.274	.0185	.064	.271	.0231	.079	.291	.0295	.119	.324	.0305	.167	.386	.0336
6	.127	.340	.0424	.143	.350	.0461	.214	.409	.0504	.278	.419	.0600	.326	.481	.0678
9	.278	.412	.0682	.294	.435	.0691	.334	.487	.0799	.445	.524	.0922	.492	.609	.1200
-3	.0556	.274	.0185	.064	.271	.0231	.079	.291	.0295	.119	.324	.0305	.167	.386	.0336
-6	.127	.340	.0424	.143	.350	.0461	.214	.409	.0504	.278	.419	.0600	.326	.481	.0678
-9	.278	.412	.0682	.294	.435	.0691	.334	.487	.0799	.445	.524	.0922	.492	.609	.1200

TABLE IV

AERODYNAMIC CHARACTERISTICS

SPHEROIDAL BODIES OF REVOLUTION

α	1/d 2			1/d 4			1/d 6			1/d 8			1/d 10		
	C_L	C_D	C_M	C_L	C_D	C_M	C_L	C_D	C_M	C_L	C_D	C_M	C_L	C_D	C_M
0	0	.196	0	0	.108	0	0	.098	0	0	.108	0	0	.134	0
3	.0635	.228	.0203	.079	.140	.0153	.091	.135	.0308	.098	.153	.0461	.103	.179	.0461
6	.167	.238	.0369	.198	.192	.0499	.214	.192	.0690	.230	.215	.0868	.246	.239	.0908
9	.214	.261	.0296	.238	.254	.0975	.278	.259	.1120	.318	.284	.125	.357	.301	.1320
-3	.0635	.228	.0203	.079	.140	.0153	.091	.135	.0308	.098	.153	.0461	.103	.179	.0461
-6	.167	.238	.0369	.198	.192	.0499	.214	.192	.0690	.230	.215	.0868	.246	.239	.0908
-9	.214	.261	.0296	.238	.254	.0975	.278	.259	.1120	.318	.284	.125	.357	.301	.1320

TABLE V

EFFECT OF VARIATION IN LENGTH/DIAMETER RATIO

ON COEFFICIENT OF DRAG AT ZERO ANGLE OF ATTACK

CYLINDRICAL BLUFF NOSES		CYLINDRICAL CONICAL NOSES		CYLINDRICAL HEMISPHERICAL NOSES		SPHEROIDAL	
1/d	C_D	1/d	C_D	1/d	C_D	1/d	C_D
2	.820	2	.484	2	.229	2	.196
4	.878	4	.474	4	.219	4	.108
6	.929	6	.494	6	.226	6	.098
8	.966	8	.530	8	.255	8	.108
10	.991	10	.572	10	.311	10	.134

APPENDIX III

FIGURES

FIGURE 1

FORCE DIAGRAM OF TYPICAL BODY OF REVOLUTION TESTED IN SMALL WIND TUNNEL

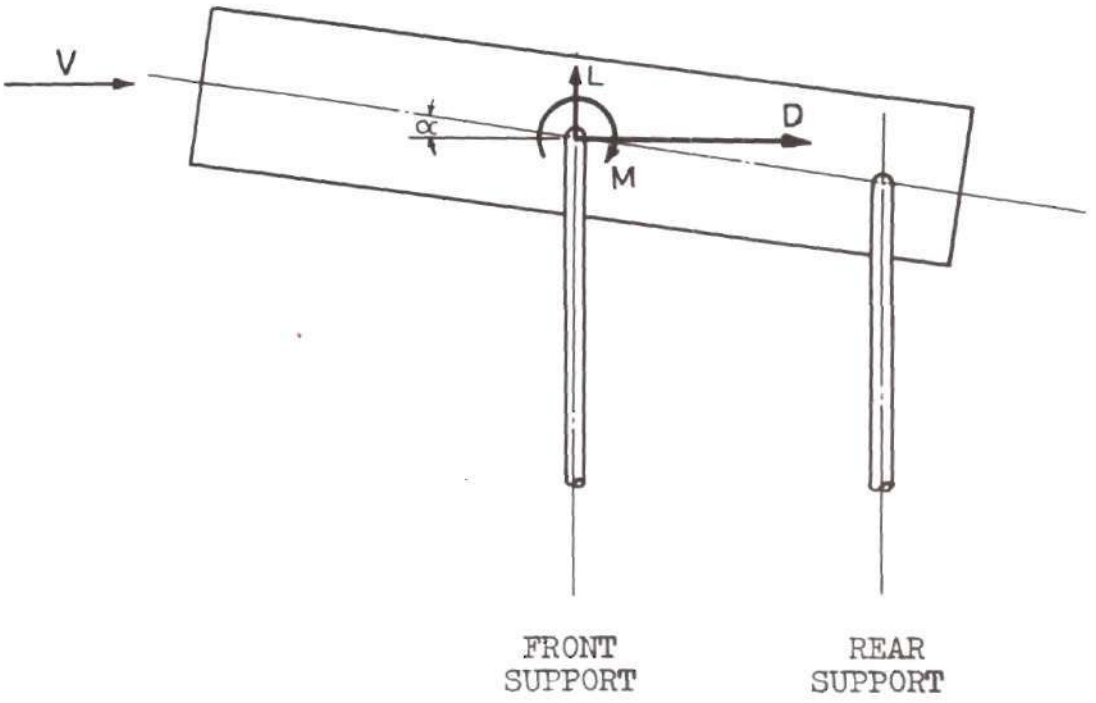

FIGURE 2

COMPARISON OF CONVENTIONAL AND OFFSET MOUNTS

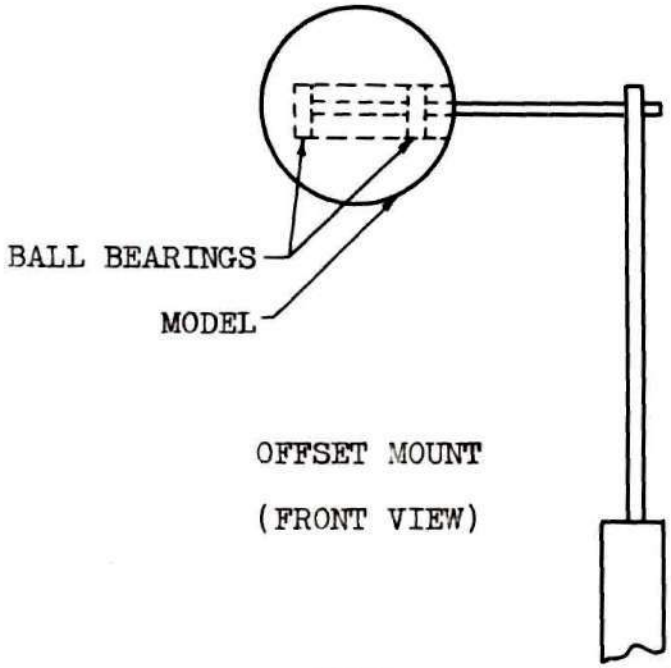

OFFSET MOUNT

(FRONT VIEW)

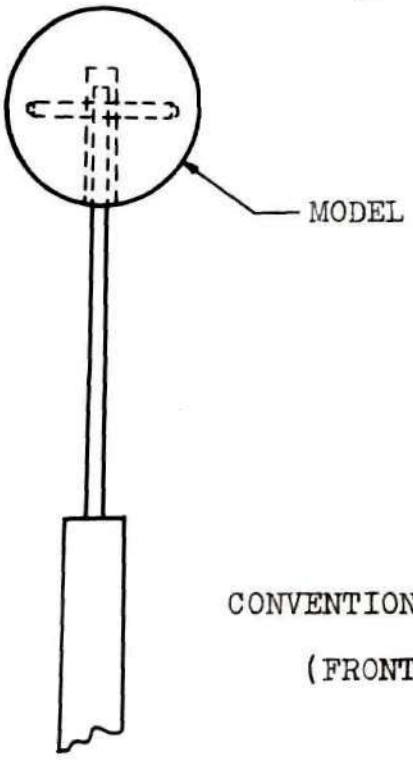

CONVENTIONAL MOUNT

(FRONT VIEW)

FIGURE 3

DRAG COEFFICIENTS FOR CYLINDRICAL BODIES OF REVOLUTION, BLUFF NOSES

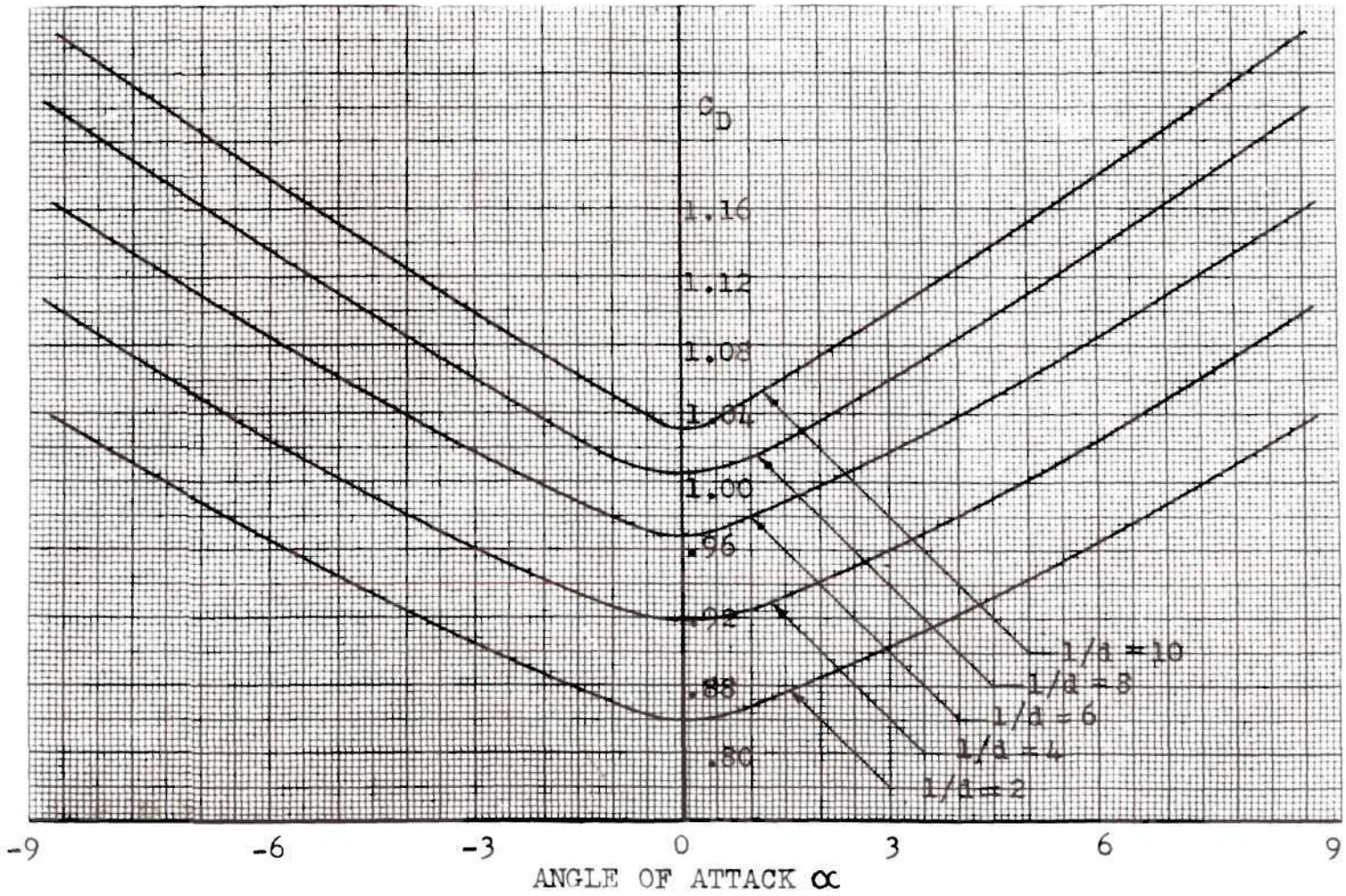

FIGURE 4

LIFT COEFFICIENTS FOR CYLINDRICAL BODIES OF REVOLUTION, BLUFF NOSES

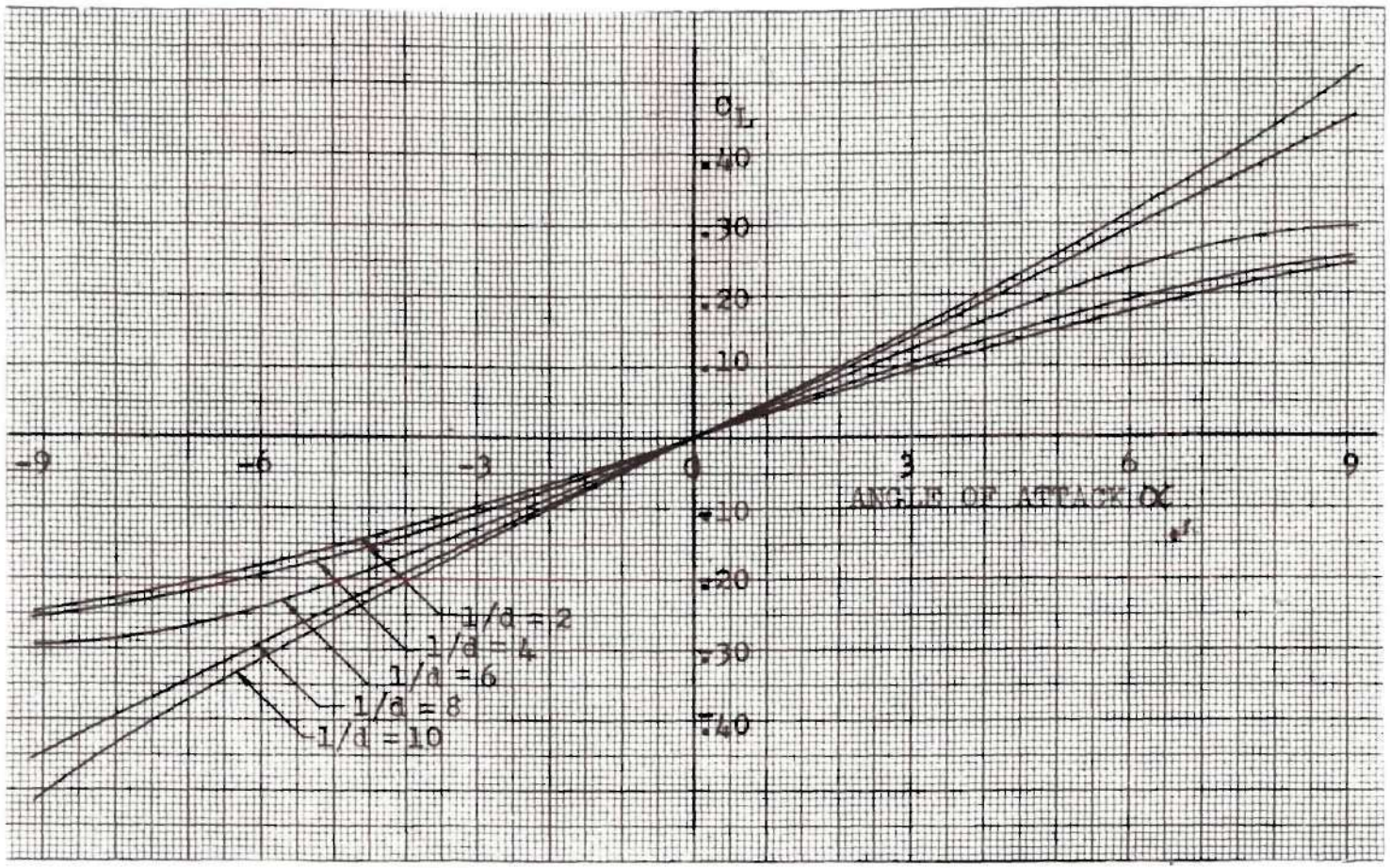

FIGURE 5

MOMENT COEFFICIENTS FOR CYLINDRICAL BODIES OF REVOLUTION, BLUFF NOSES

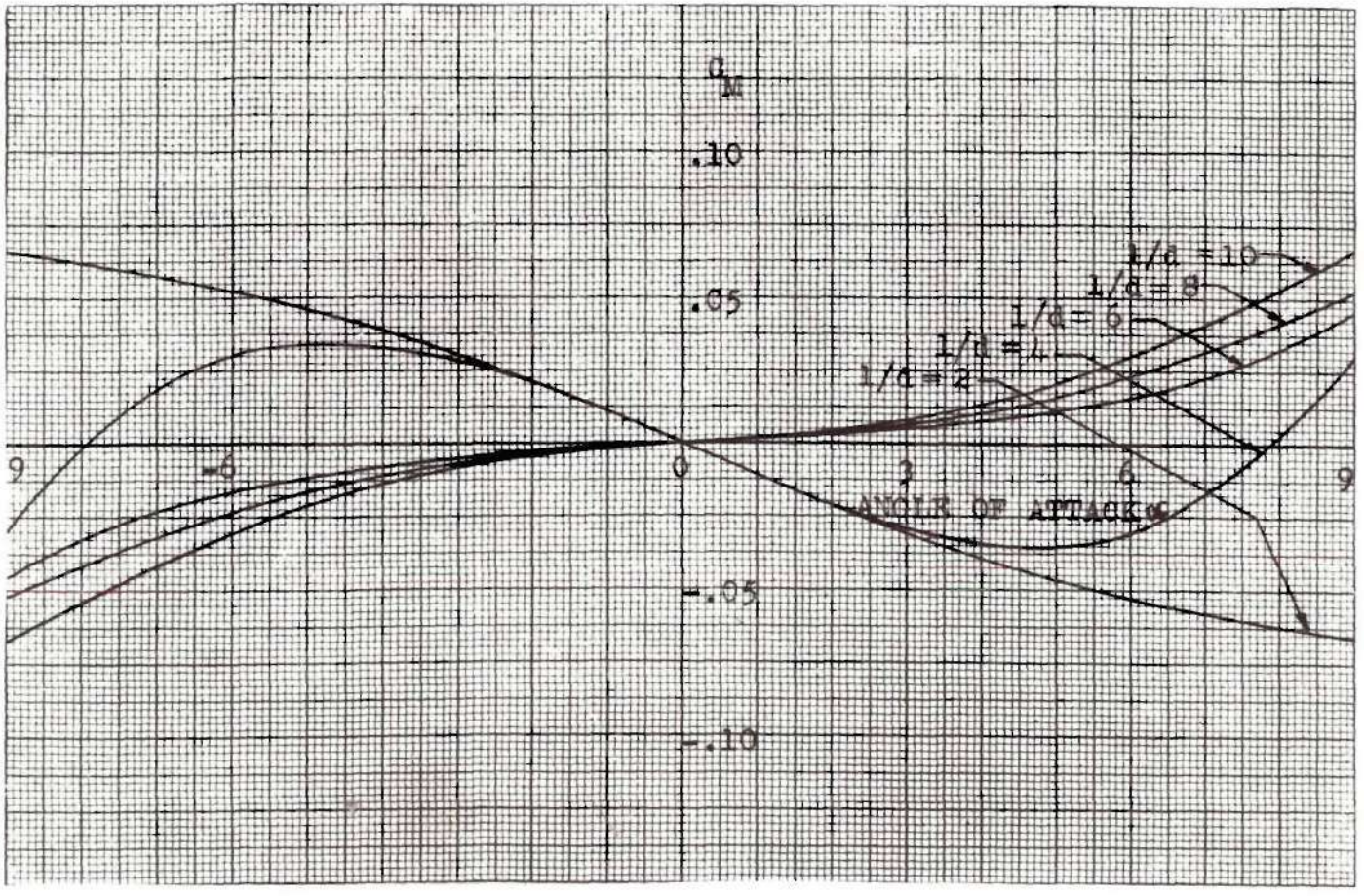

FIGURE 6

DRAG COEFFICIENTS FOR CYLINDRICAL BODIES OF REVOLUTION, CONICAL NOSES

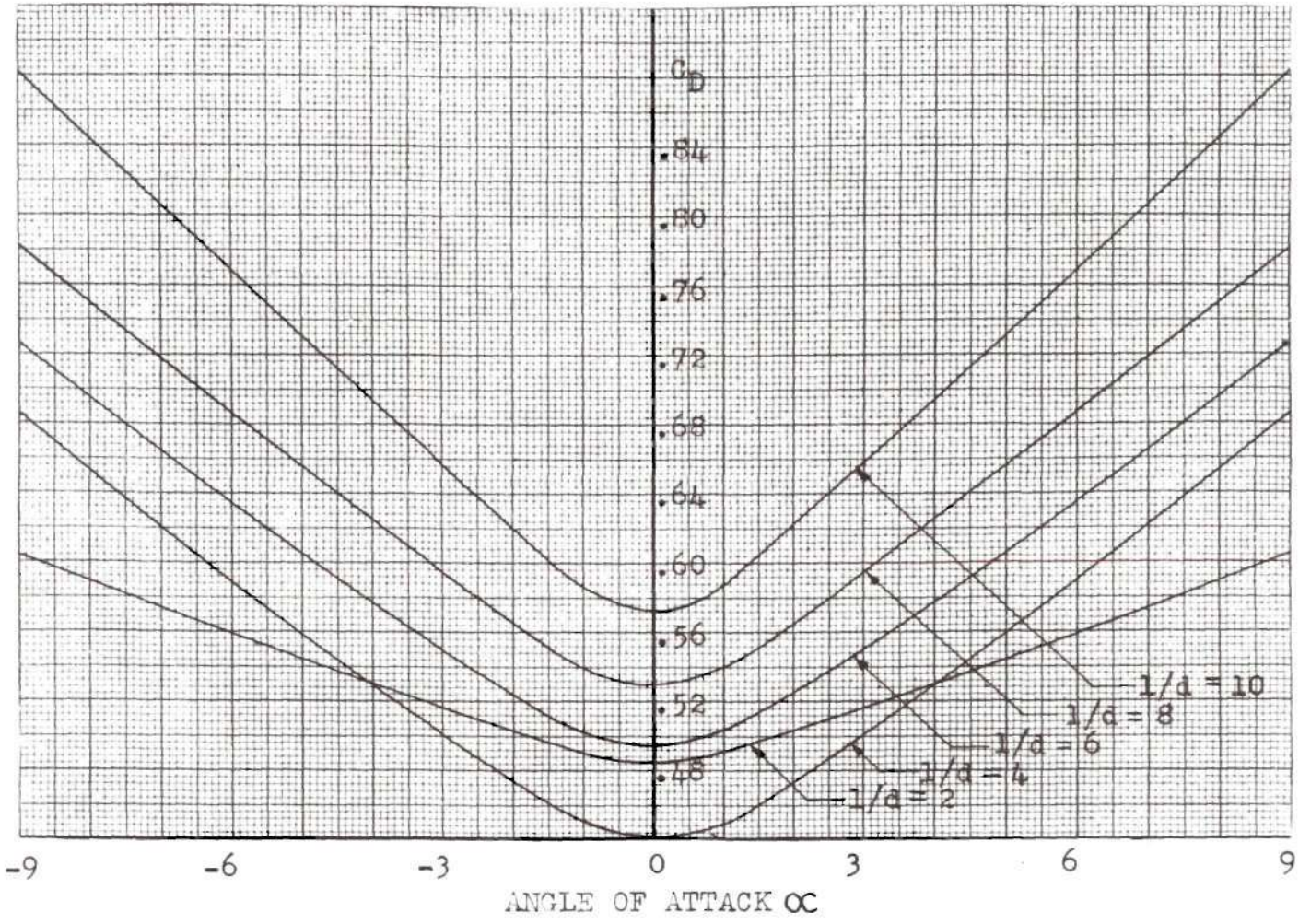

FIGURE 7

LIFT COEFFICIENTS FOR CYLINDRICAL BODIES OF REVOLUTION, CONICAL NOSES

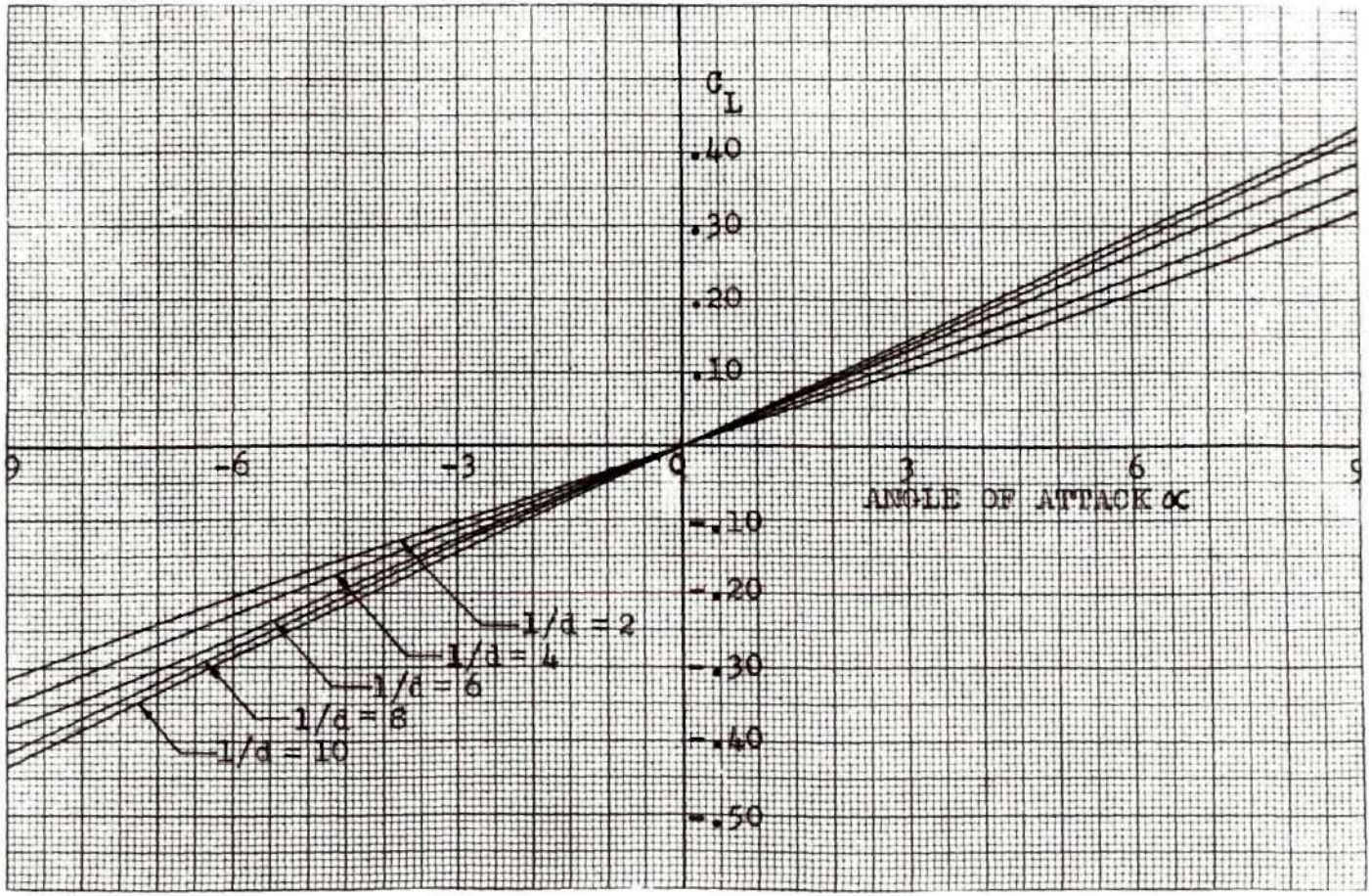

FIGURE 8

MOMENT COEFFICIENTS FOR CYLINDRICAL BODIES OF REVOLUTIONS, CONICAL NOSES

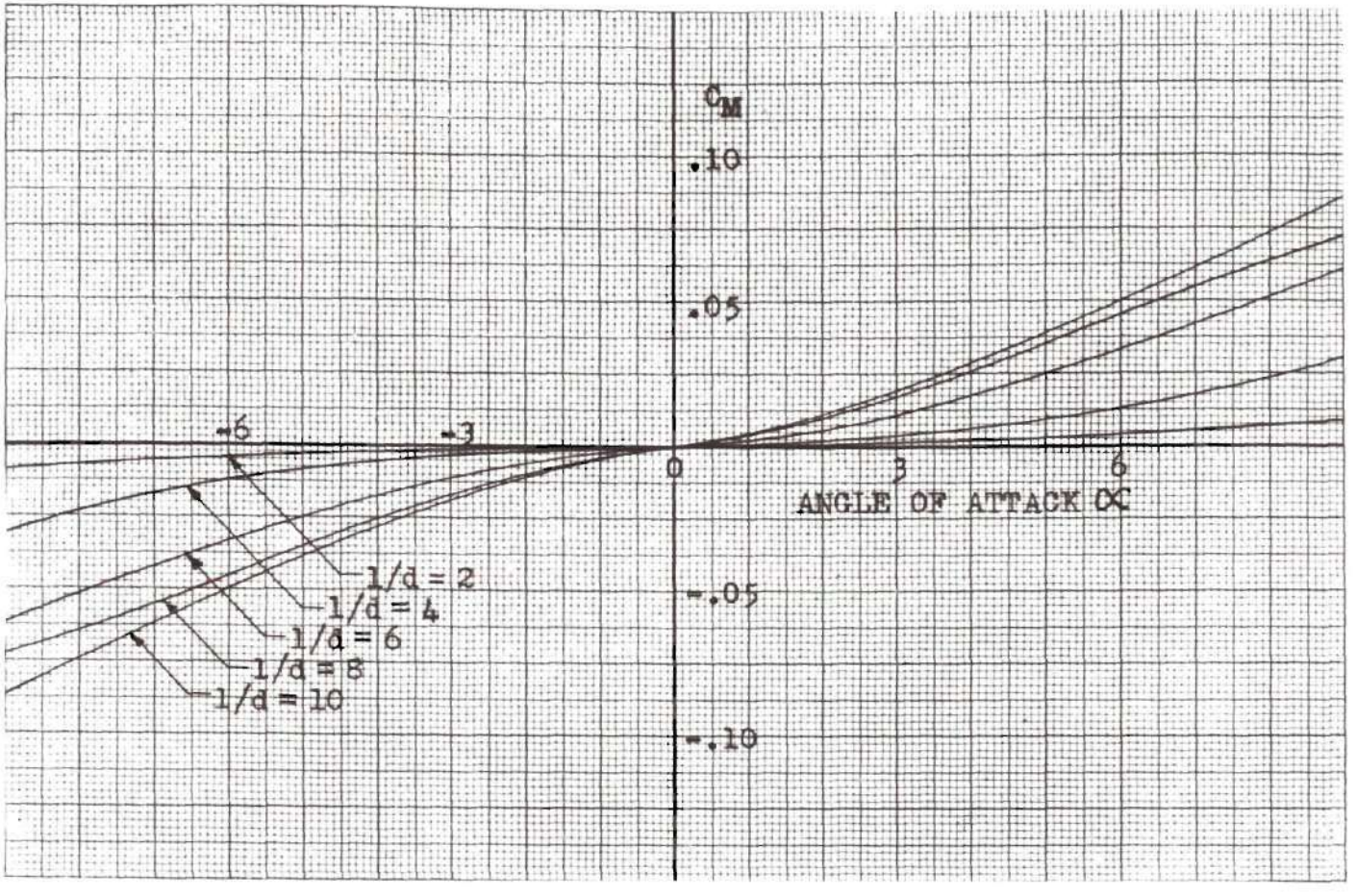

FIGURE 9

DRAG COEFFICIENTS FOR CYLINDRICAL BODIES OF REVOLUTION, HEMISPHERICAL NOSES

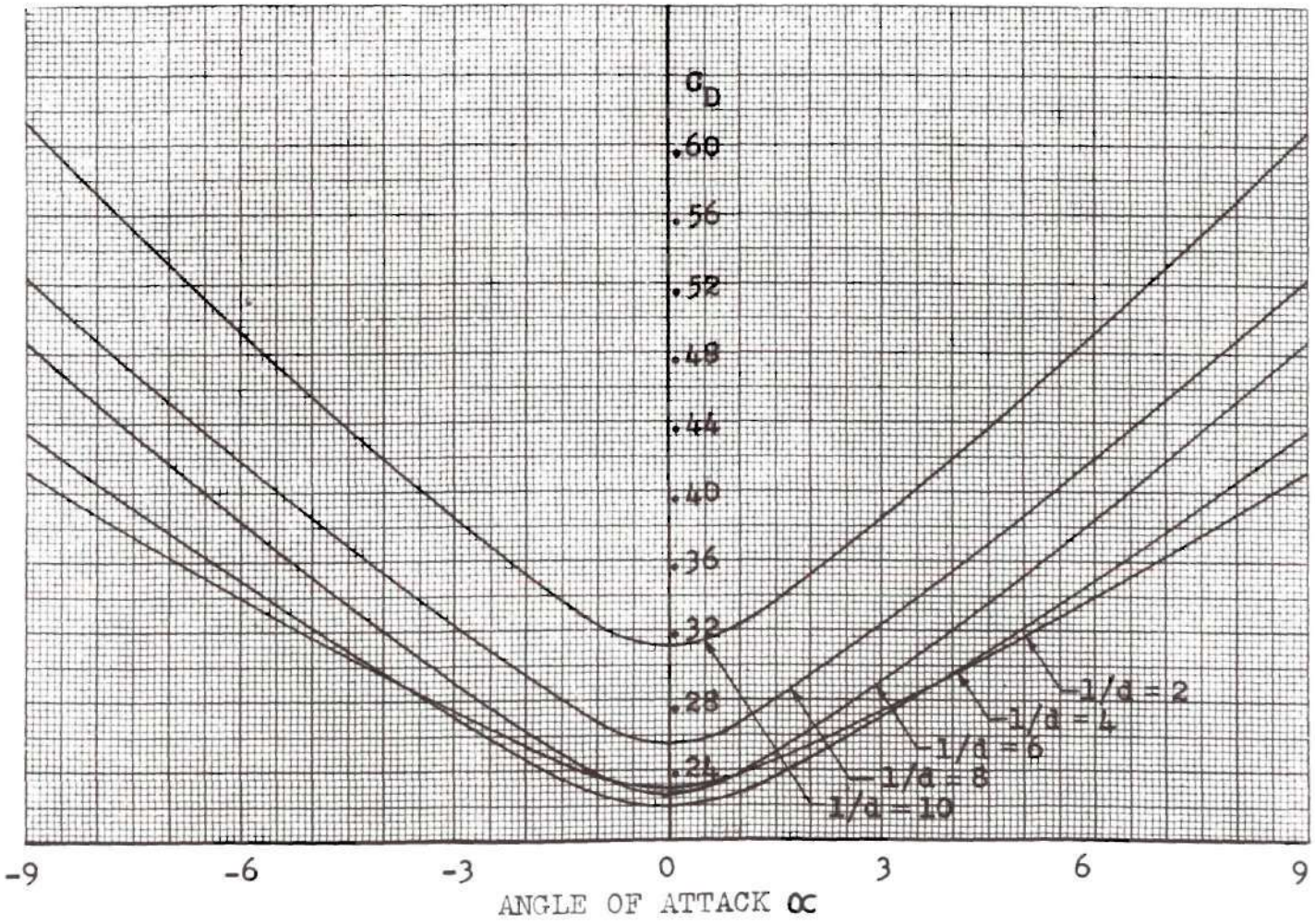

FIGURE 10

LIFT COEFFICIENTS FOR CYLINDRICAL BODIES OF REVOLUTION, HEMISPHERICAL NOSES

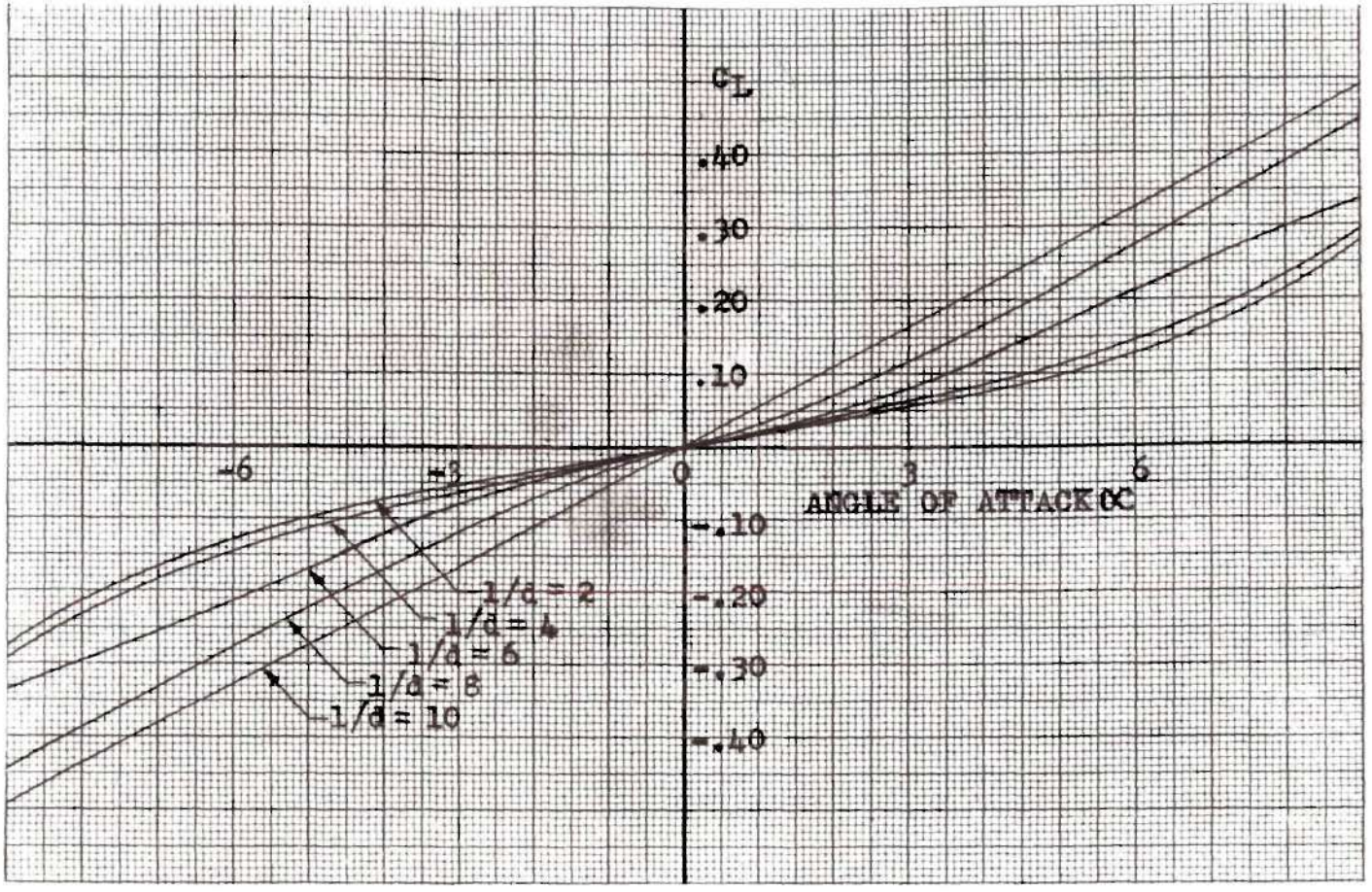

FIGURE 11

MOMENT COEFFICIENTS FOR CYLINDRICAL BODIES OF REVOLUTION, HEMISPHERICAL NOSES

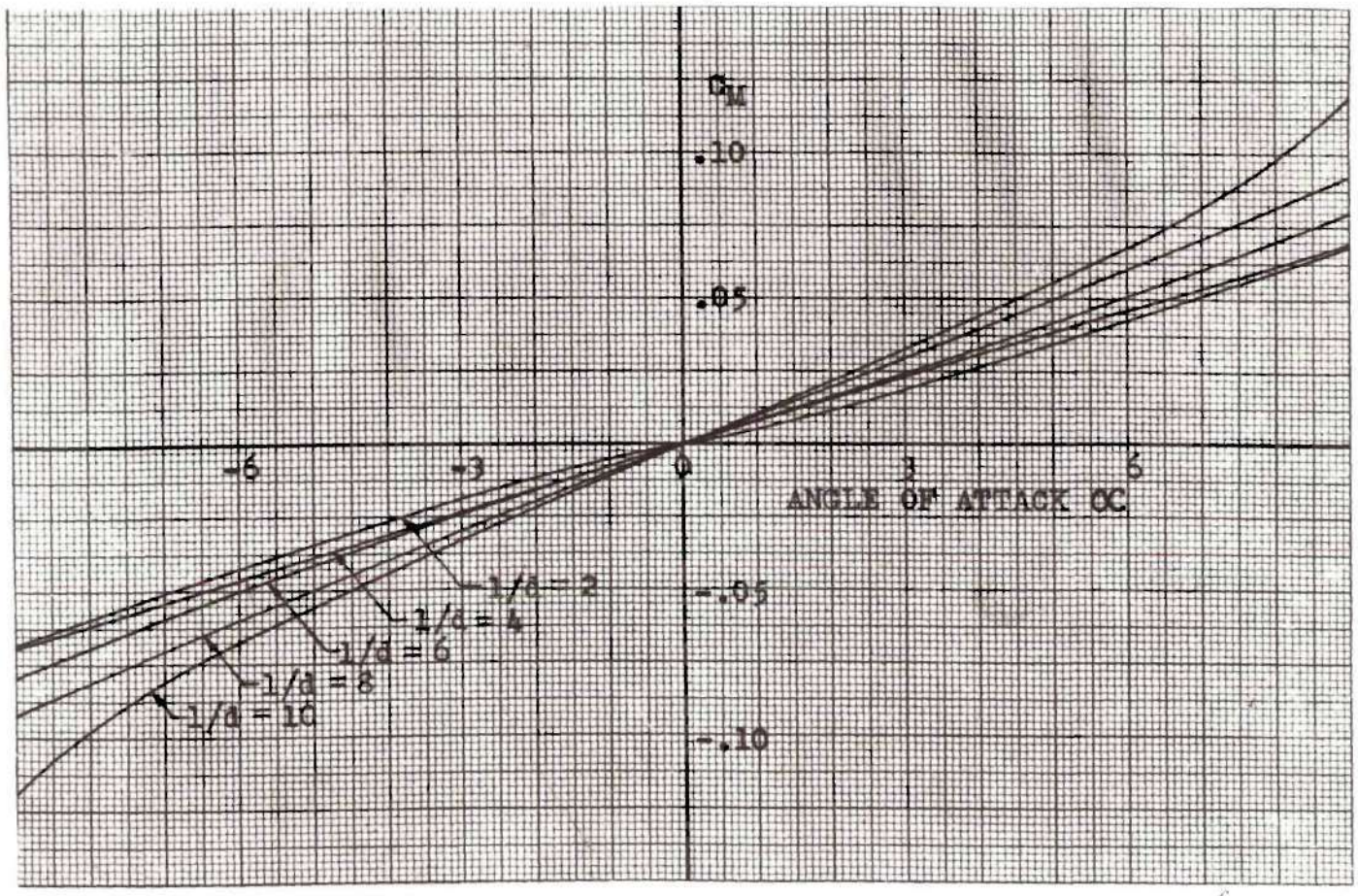

FIGURE 12

DRAG COEFFICIENTS FOR SPHEROIDAL BODIES OF REVOLUTION

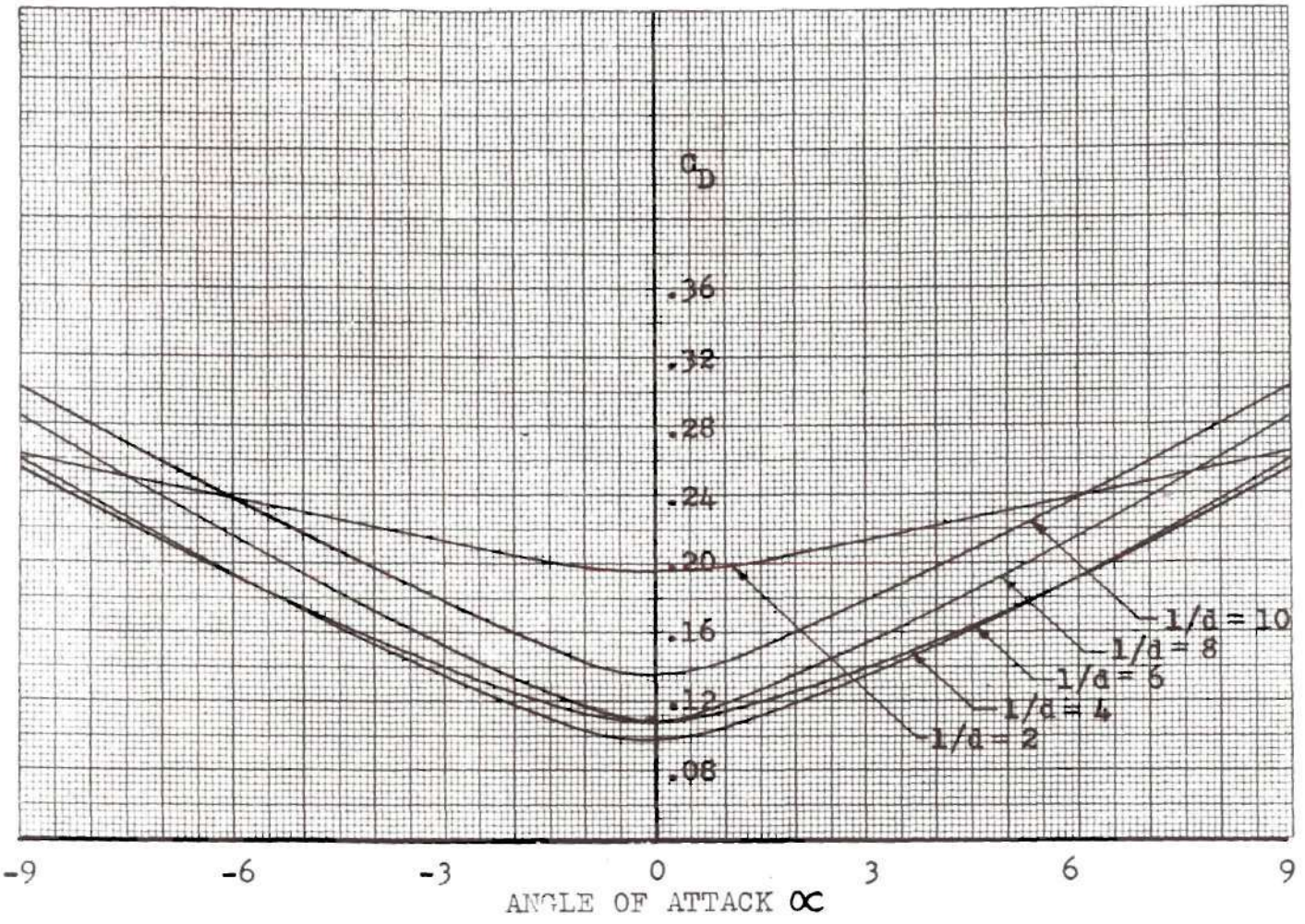

FIGURE 13

LIFT COEFFICIENTS FOR SPHEROIDAL BODIES OF REVOLUTION

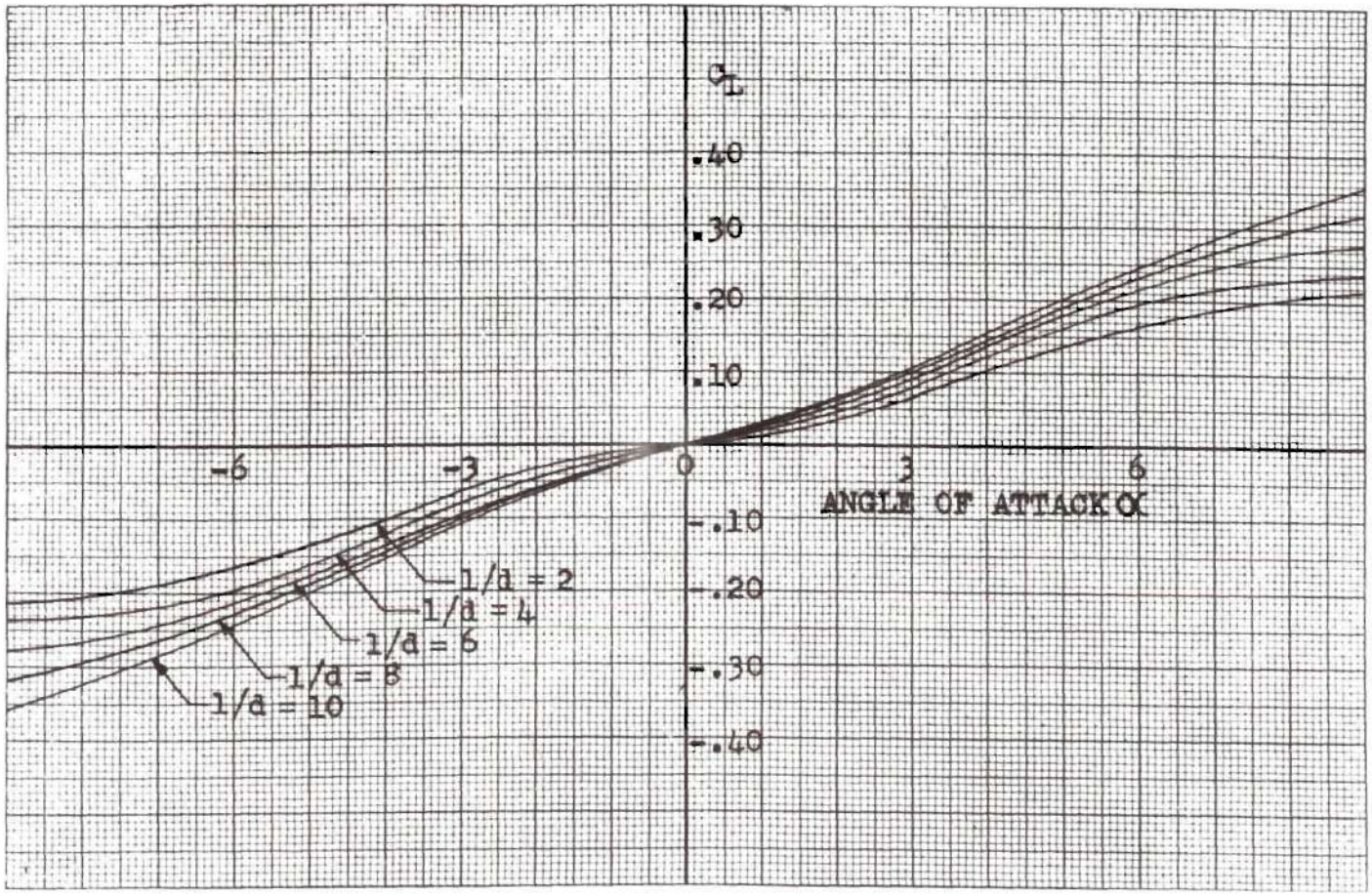

FIGURE 14

MOMENT COEFFICIENTS FOR SPHEROIDAL BODIES OF REVOLUTION

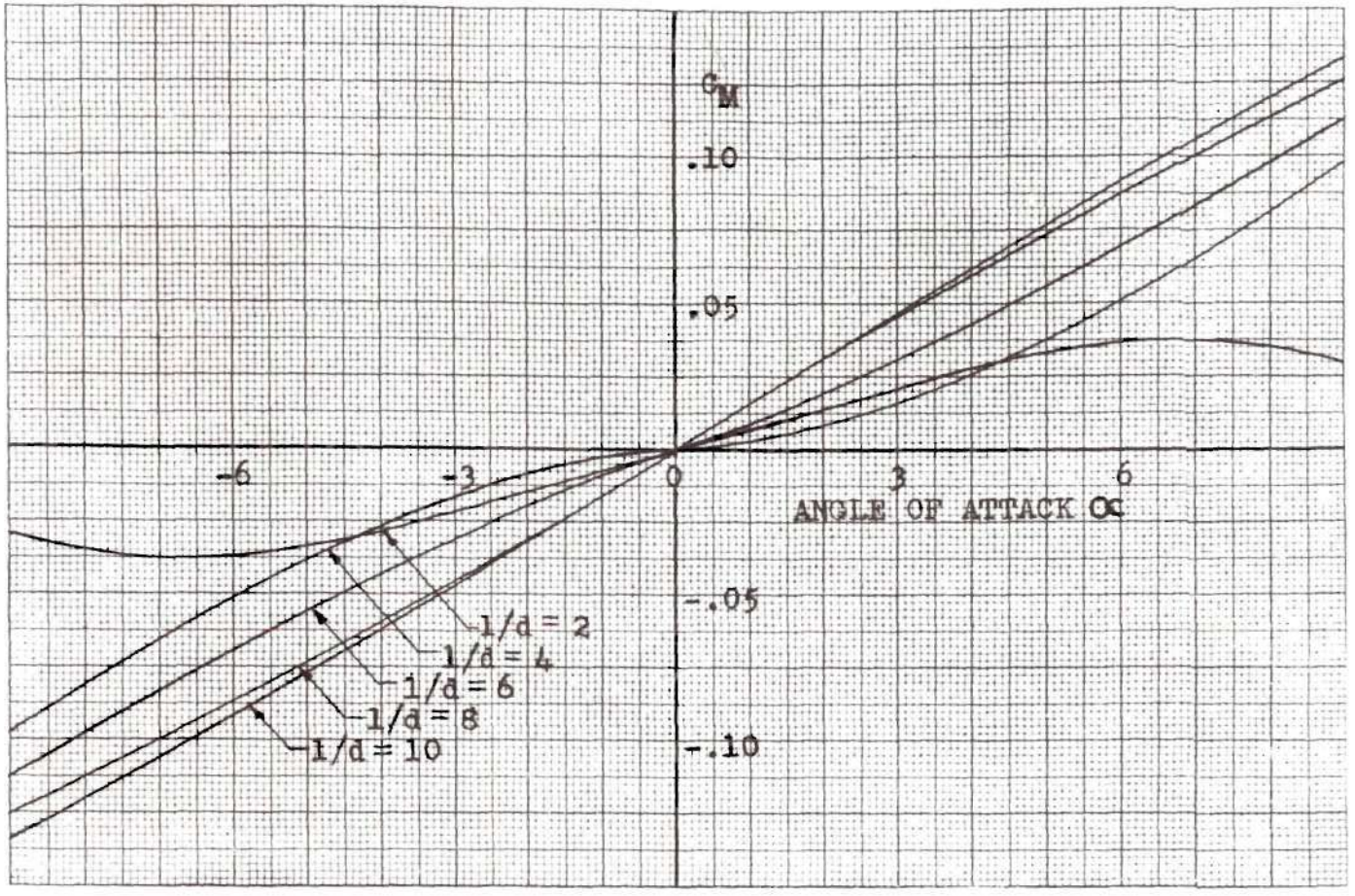

FIGURE 15

COMPARISON OF DRAG COEFFICIENTS AT ZERO ANGLE OF ATTACK FOR DIFFERENT BODIES OF REVOLUTION

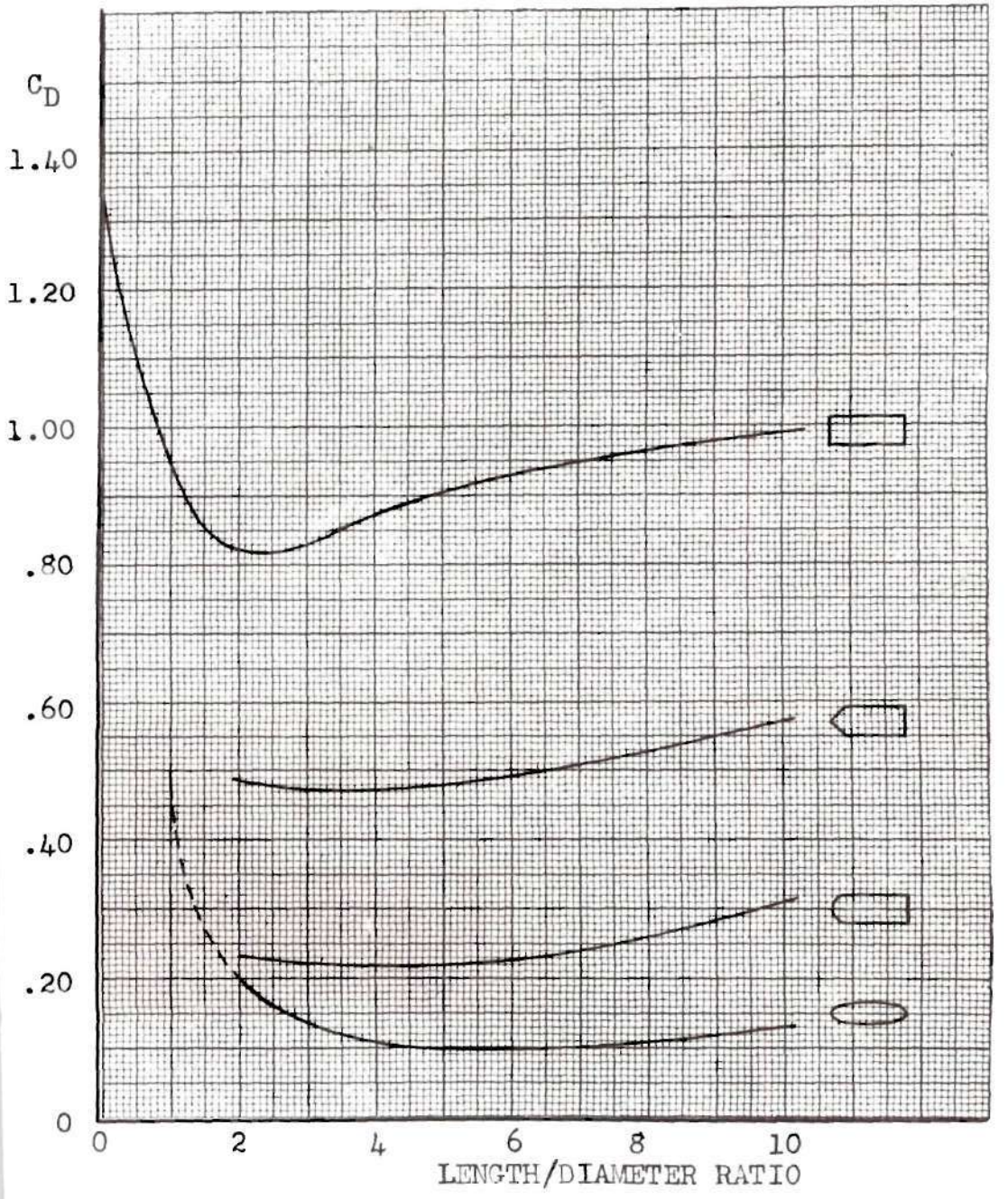

FIGURE 16

COMPARISON OF PRESENT EXPERIMENTAL DRAG COEFFICIENTS

OF BLUFF CYLINDERS WITH EIFFELS' TEST VALUES

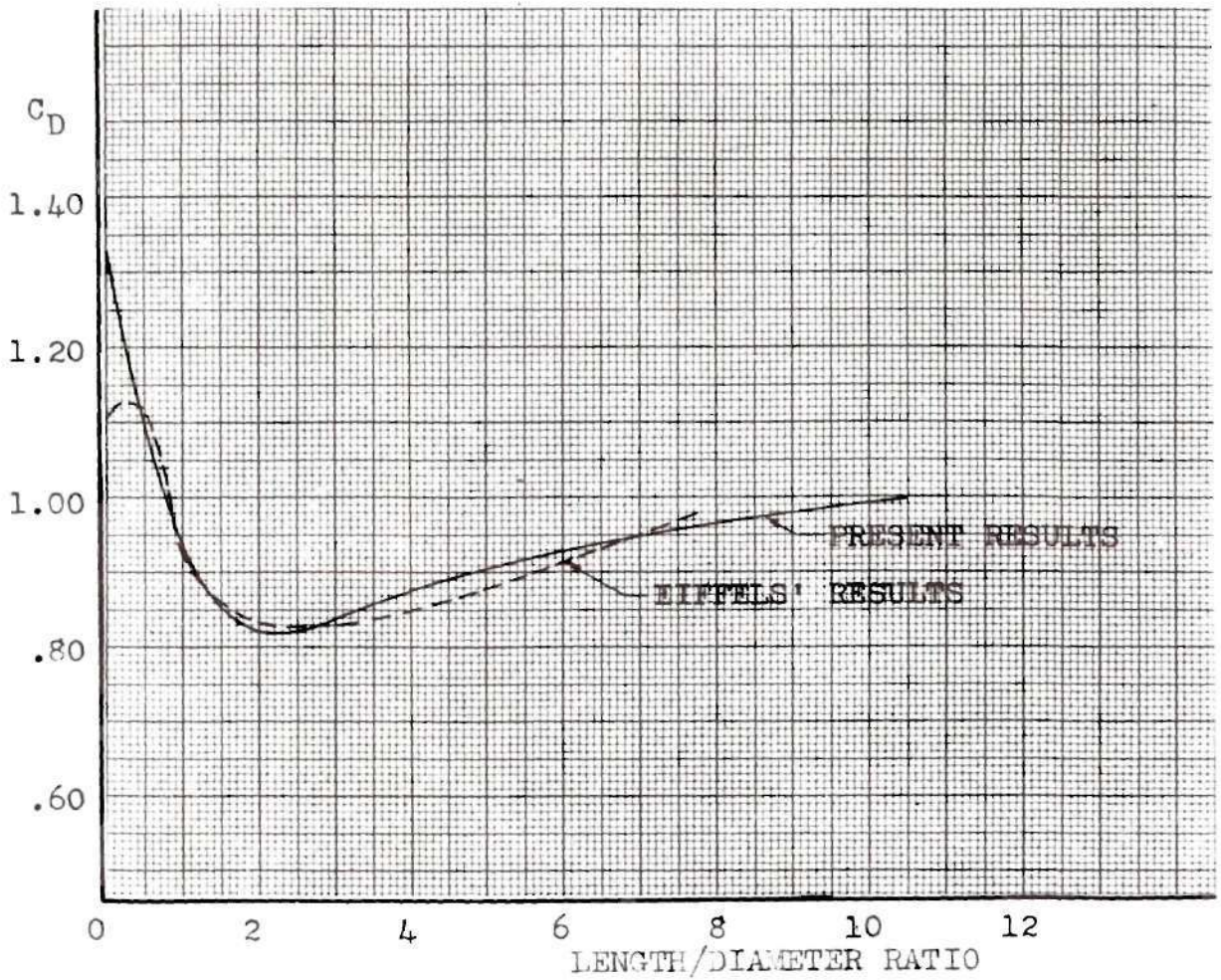

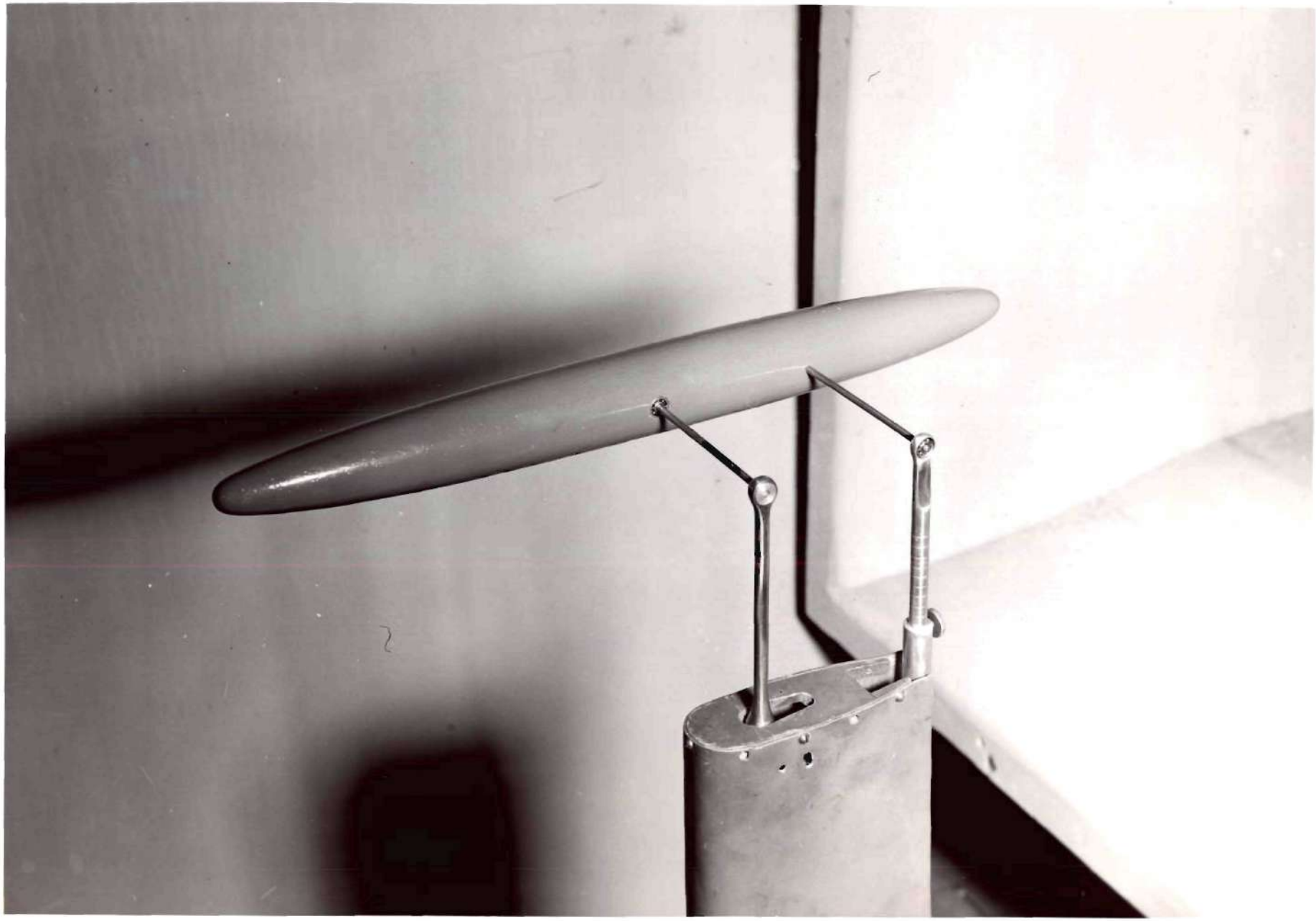

FIG.17 MODEL INSTALLATION ON BALANCE SYSTEM

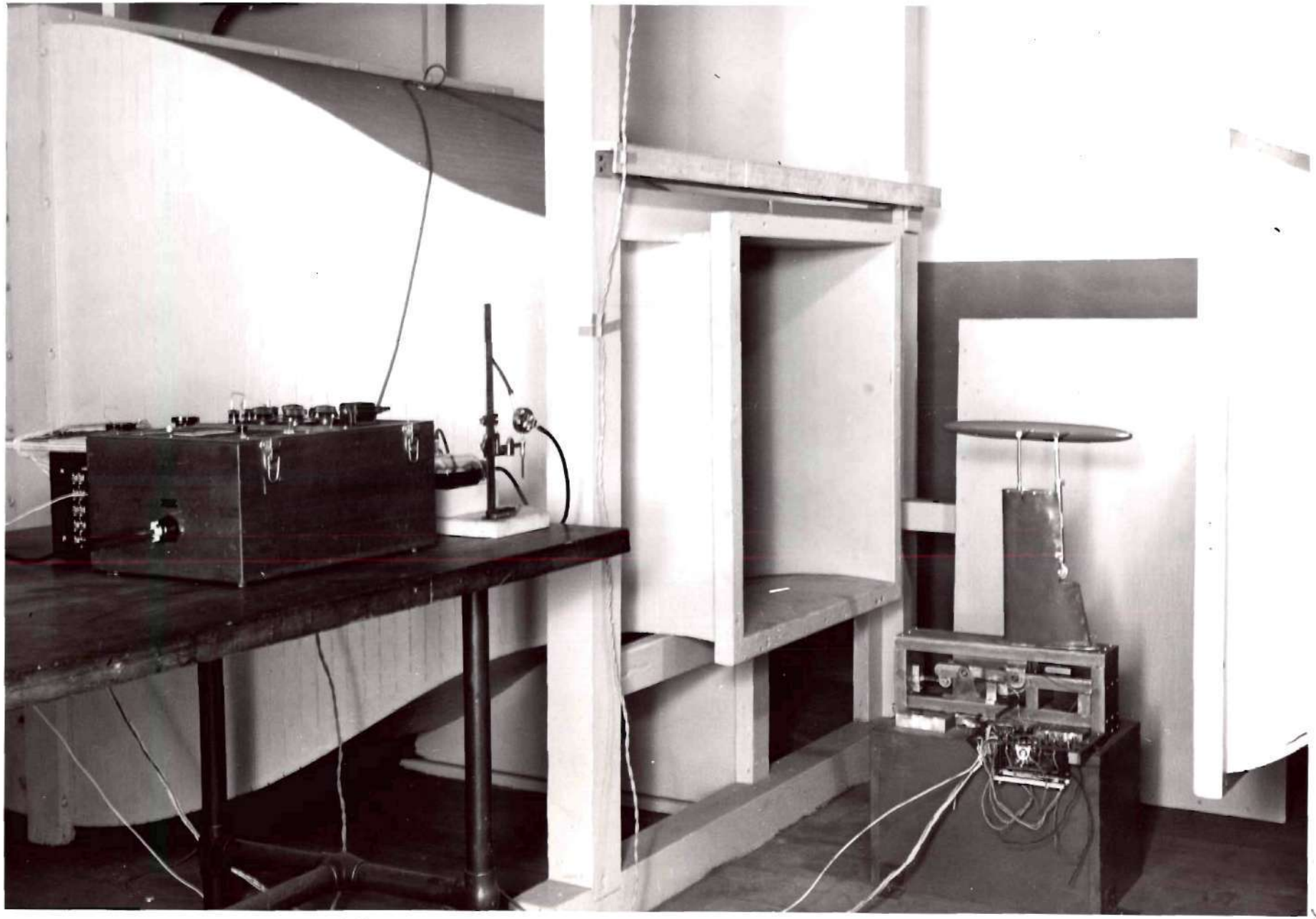

FIG. 18 TEST-SECTION AND APPARATUS

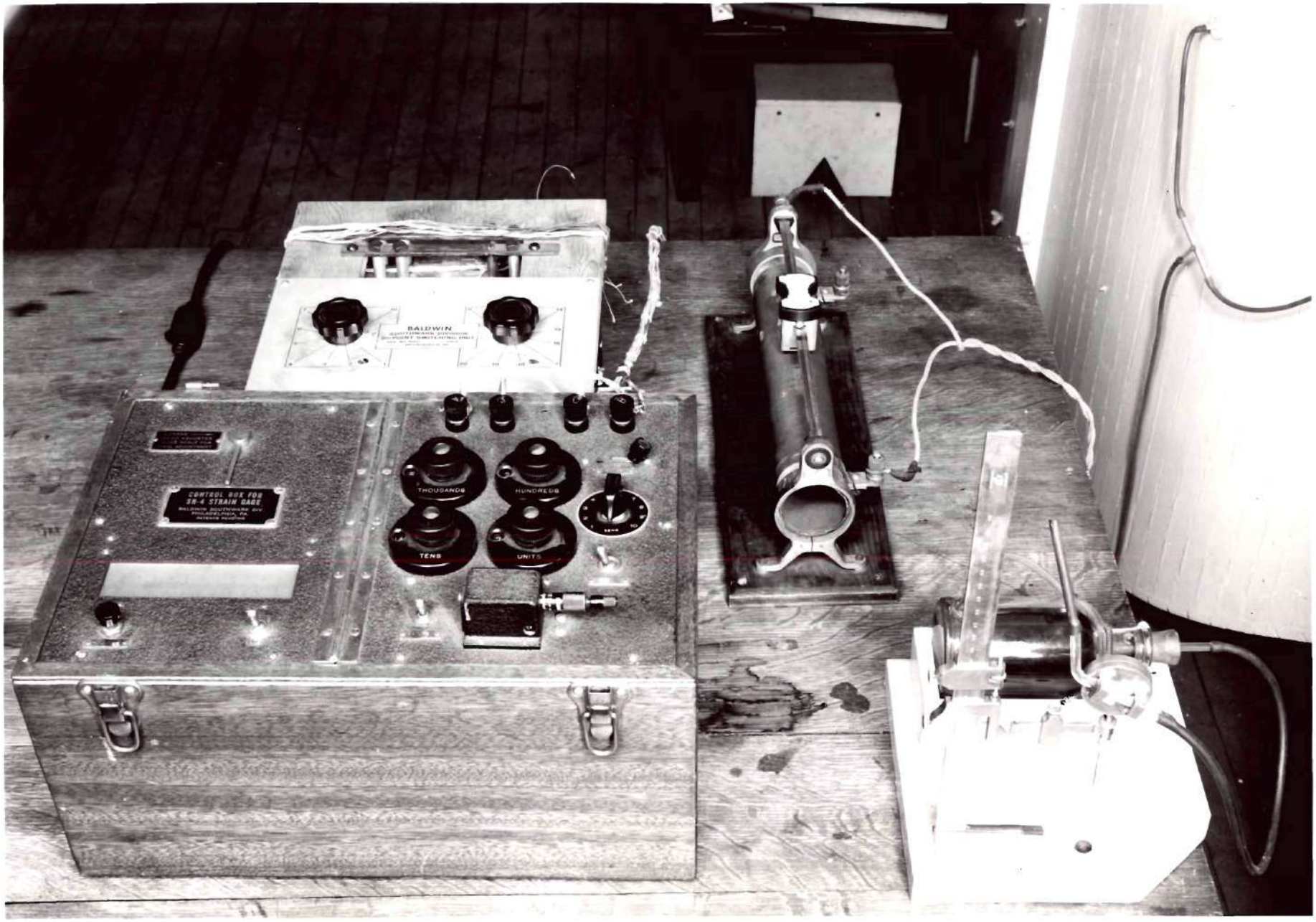

FIG. 19 CONTROL AND INDICATING APPARATUS

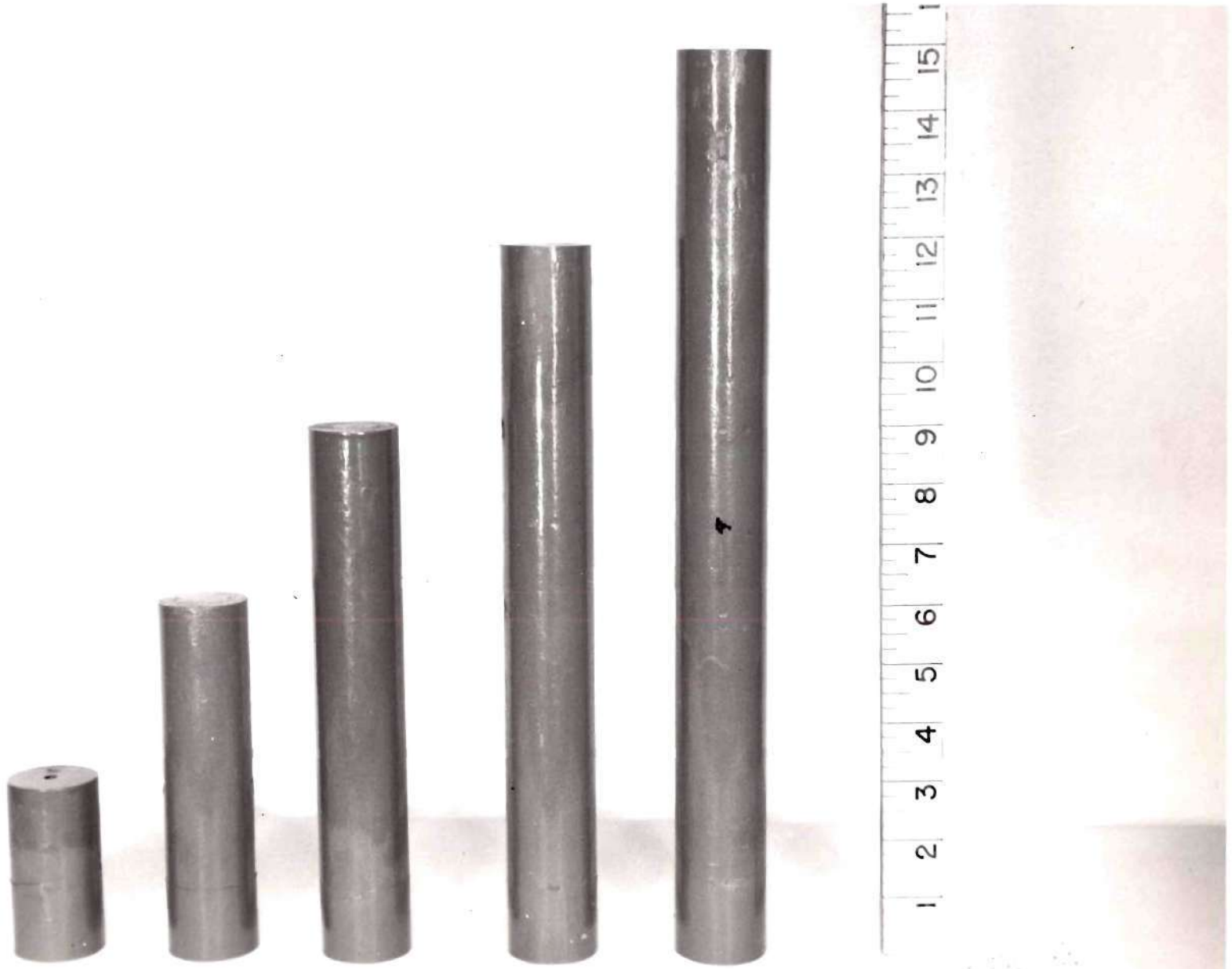

FIG.20 CYLINDRICAL BODIES OF REVOLUTION, BLUFF NOSES

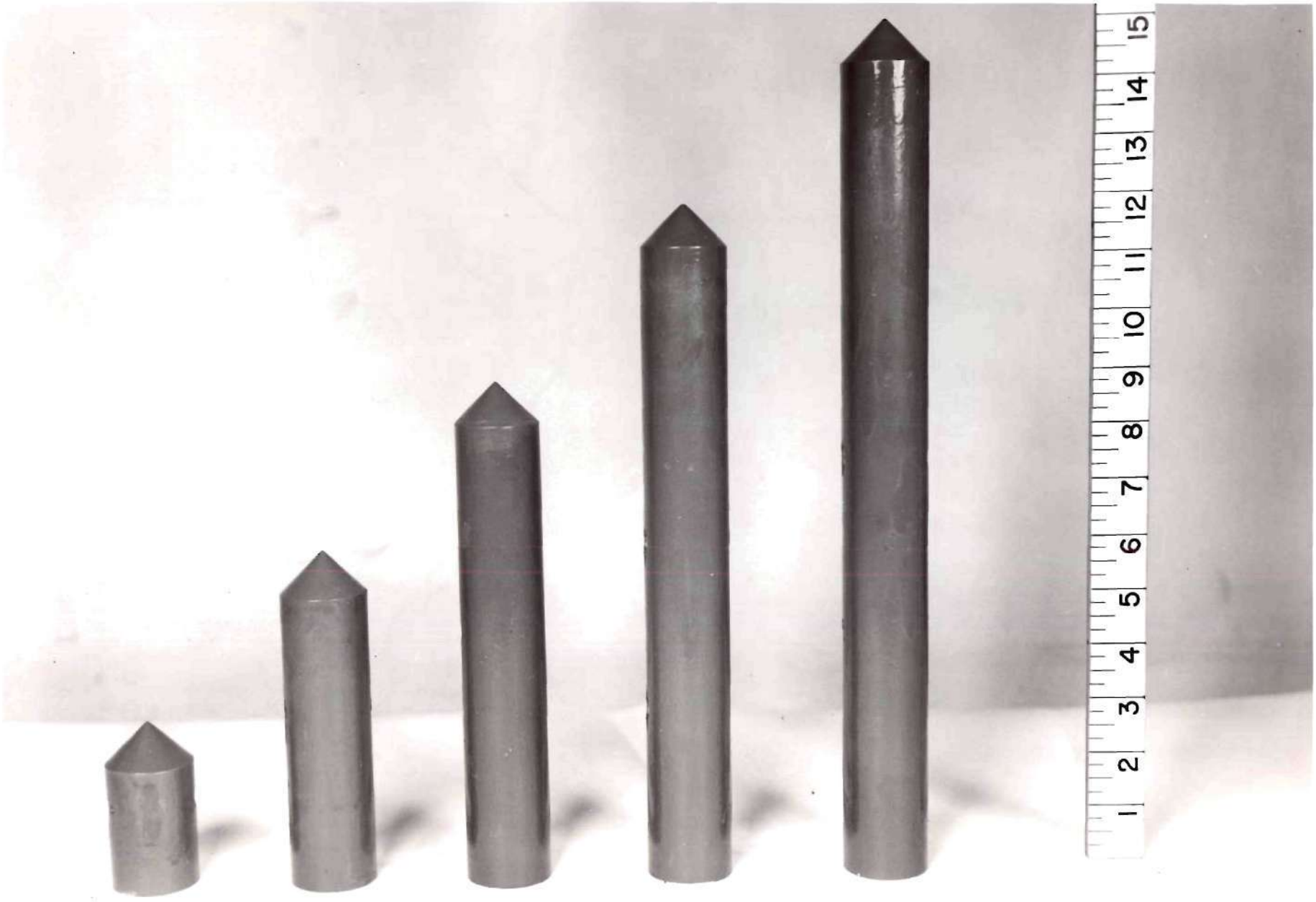

FIG. 21 CYLINDRICAL BODIES OF REVOLUTION, CONICAL NOSES

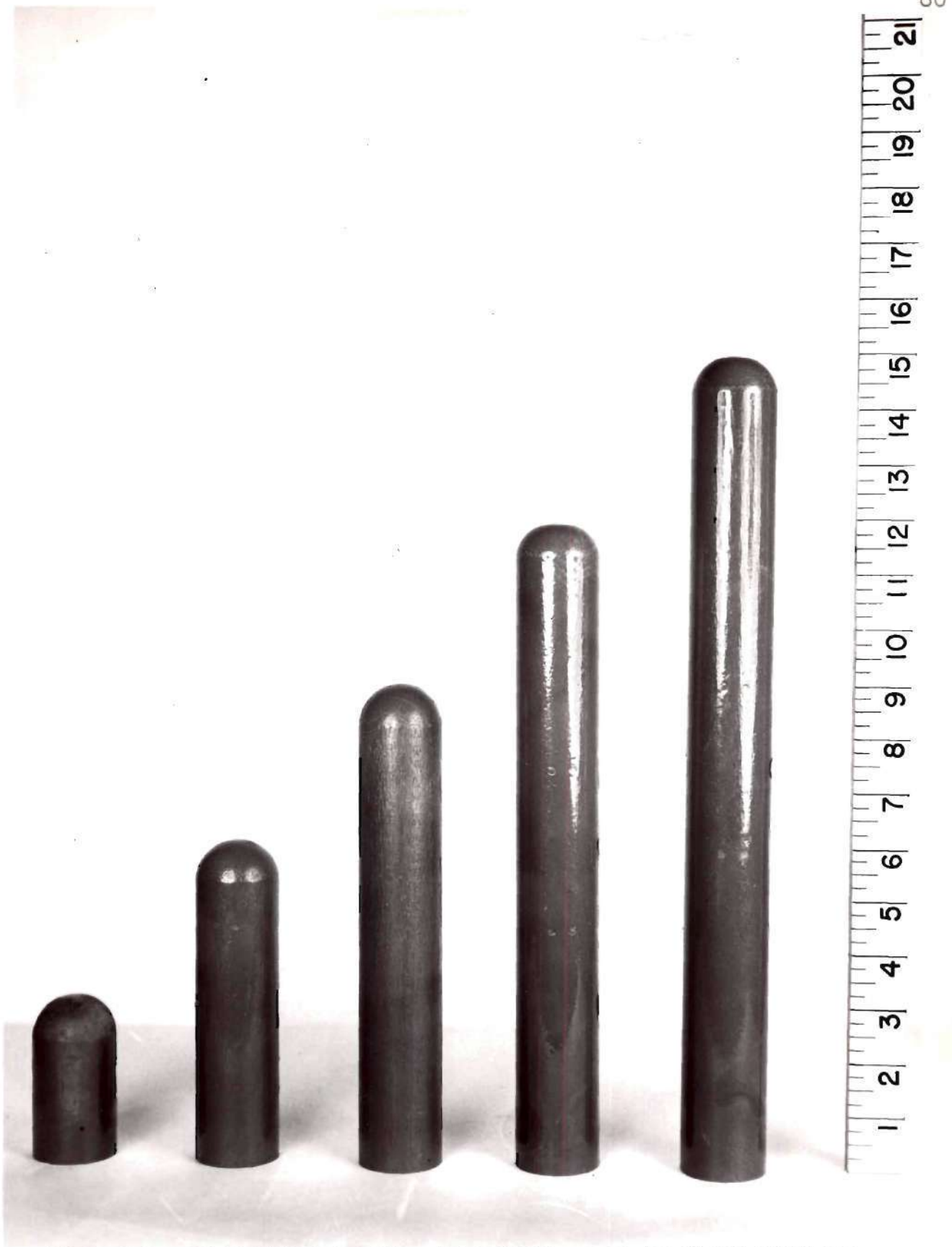

FIG. 22 CYLINDRICAL BODIES OF REVOLUTION

HEMISPHERICAL NOSES

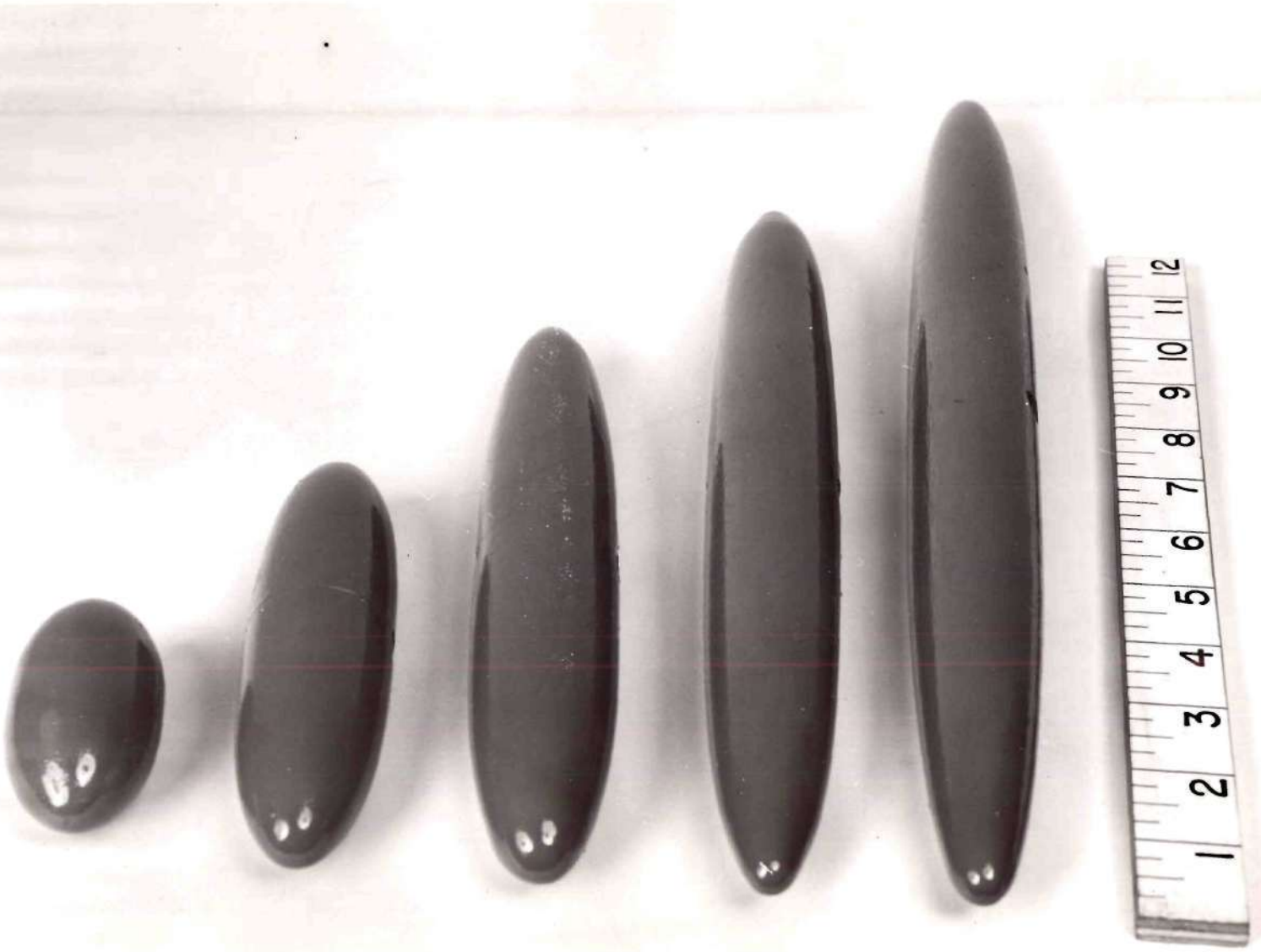

FIG. 23 SPHEROIDAL BODIES OF REVOLUTION